SCOUR AROUND CIRCULAR BRIDGE PIERS AT HIGH FROUDE NUMBERS

by

Subhash C. Jain and Edward E. Fischer

Sponsored by
U.S. Department of Transportation

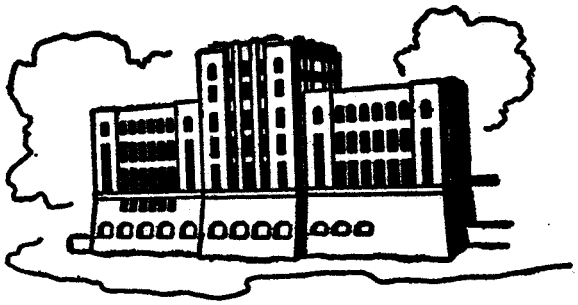

IIHR Report No. 220

Iowa Institute of Hydraulic Research
The University of Iowa
Iowa City, Iowa

December 1979

SCOUR AROUND CIRCULAR BRIDGE PIERS AT HIGH FROUDE NUMBERS

by

Subhash C. Jain and Edward E. Fischer

Sponsored by
U.S. Department of Transportation

IIHR Report No. 220.

Iowa Institute of Hydraulic Research
The University of Iowa
Iowa City, Iowa

December 1979

ABSTRACT

The results of laboratory experiments on scour around circular piers in cohesionless bed material at high flow velocities, U, are presented. The scour depth in the sediment transport regime ($U > U_c$, where U_c is the velocity for the initiation of sediment movement) first decreases and then increases with increasing velocity. A formula to predict scour depth for flows with Froude number, F ($F = U/\sqrt{gy}$ where y is the flow depth and g is the gravitational constant), such that $F - F_c \geq 0.15$ ($F_c = U_c/\sqrt{gy}$) is developed. Some existing predictors of local scour are presented and their limitations discussed, and a new formula to predict maximum clearwater scour is proposed.

ACKNOWLEDGEMENT

This study was sponsored by the United States Department of Transportation under contract number DOT-FH-11-9276.

TABLE OF CONTENTS

LIST OF TABLES

LIST OF FIGURES

LIST OF SYMBOLS

Symbol	Definition	Dimensions	Units
A, A_1, A_2, B	Empirically determined coefficients.		
a_r	A function of boundary Reynolds number in logarithmic velocity distribution law		
b	Horizontal pier width	L	cm
d_s	Scour depth below mean bed elevation	L	cm
D	Mean sediment size	L	mm
F	Froude number		
F_c	Critical Froude number for incipient sediment motion		
F_d	Particle Froude number		
F_{dc}	Critical particle Froude number for incipient sediment motion		
g	Acceleration due to gravity	L/t^2	cm/sec^2
ℓ	Pier length parallel to approach flow	L	
m, n, p, r	Empirically determined exponents		
t	Time	t	sec
U	Average critical velocity for initiation of sediment movement	L/t	m/sec
y	Average depth of approach flow	L	cm
α_1, α_2, β_1, β_2	Empirically determined exponents		
γ_s'	Submerged specific weight of sediment	m/L^2t^2	gr/cm^2sec^2

LIST OF SYMBOLS (CONTINUED)

Symbol	Definition	Dimensions	Units
ν	Ambient fluid kinematic viscosity	L^2/t	cm^2/sec
ρ	Ambient fluid density	M/L^3	gr/cm^3
ρ_s	Sediment density	M/L^3	gr/cm^3
σ_g	Geometric distribution of sediment size about the mean		
ϕ	Pier shape factor		

I. INTRODUCTION

The safe and economical design of bridge piers requires accurate prediction of the maximum expected depths of scour of the stream bed around them. The interaction between the flow around a bridge pier and the erodible sediment bed surrounding it is very complex. In fact, the phenomenon is so involved that only very limited success has been enjoyed by the attempts to model scour computationally, and physical models remain the principal tool employed for estimating expected depths of scour.

There are three factors which intervene to change bed elevations at bridge sites. First, there may be a general aggredation or degradation of the river bed, which accompanies changes in the water and sediment discharges of the stream. Second, there may be scour due to shifting and migration of bed forms (dunes, antidunes, bars, etc) and river banks. Third, the higher local velocities produced by the presence of the pier and the resulting constriction and obstruction of the flow create local scour around the pier. Scour depths due to the first two factors may occur regardless of a bridge crossing. Though the conceptual separation of the three scour processes is helpful in understanding the entire scour problem, these processes are not completely independent.

This study is primarily concerned with the local scour that occurs around bridge piers. Two types of scour may be identified; (1) clear-water scour - where material is removed from the scour hole and not replaced, and (2) scour - that occurs with general sediment transport. Scour at the pier due to the presence of the pier alone can be investigated in the clearwater regime only. In the sediment-transport regime, scour at the pier occurs due to changes in the flow pattern produced by both the pier and the bed forms. It is not possible to separate the contributions of the two factors to the scour as the interaction of the velocity fields generated by them is very intricate.

Following the experimental study of Chabert and Engeldinger (1956) on local scour around bridge piers, most of the investigators in this area concurred on the general shape of the curve which delineates the variation of scour depth with mean flow velocity. According to this curve, scour depth increases with increase in mean velocity in the clear-water regime, reaches an absolute maximum at a velocity approximately equal to the mean velocity for incipient sediment motion (hereinafter referred to as the threshold velocity), and decreases slightly with further increase in mean velocity in the sediment-transport regime where it fluctuates aperiodically about the equilibrium scour depth due to bed-form migration. Since the maximum scour depth is required in designing bridge piers, most of the experimental studies in the past were conducted either in the clear-water regime or with flow velocities not much higher than the threshold velocity in the sediment-transport regime. Scour due to bed forms in the latter case was considered to be insignificant in comparison to that due to the presence of the pier. Since scour depths in most experimental studies were measured after stopping the flow, it was inadvertently assumed that the change in the maximum scour around the pier due to the deposition of suspended sediment was insignificant. This presumption clearly is not true at high flow velocities as there is a lot of sediment in suspension similar to that in a river during floods.

A wide variety of empirical equations based upon a limited range of data (both laboratory and prototype) have been developed in the past to estimate the maximum scour depths around bridge piers. Unfortunately, the relatively large scatter in the available data on local scour around bridge piers makes it possible to fit a wide variety of curves which diverge greatly at high Froude numbers and high relative depths of the flow (Froude number $F = U/\sqrt{gy}$, relative depth = y/b, where U is the mean flow velocity, y is the mean flow depth, g is the acceleration due to gravity and b is the pier size). Not only that their extrapolation to higher Froude numbers and relative depths cannot be used as a sound basis for pier design, it is also difficult to draw conclusions regarding the appropriateness of these formulas at low Froude numbers and relative depths.

A. Scope of the Study. The primary objective of the present study was to gather data on scour depths obtained in flows of high Froude number to validate or invalidate the formulas based on scour depths generated at low Froude numbers. The investigation was pursued in the following stages:

(1) The existing literature on physical model studies of bridge-pier scour was reviewed and the findings were summarized in the state-of-the-art section of this report. The limitations of some of the predictors of local scour in terms of the range of parameters used in their development, the nature of the bed material, and the adequacy of the analysis in considering the impact of bed forms were discussed.

(2) A series of laboratory experiments in a flume using cylindrical piers were conducted at high Froude numbers, and the data on the depth a geometry of the scour pattern developed in cohensionless bed material were obtained. A special technique to measure the scour below the mean bed-elevation was adopted to overcome the problem of sediment deposition when the flow was stopped.

(3) The variation of the maximum scour depths with changes in flow and sediment conditions was analyzed, and a formula to predict the scour depth at higher Froude numbers was developed.

(4) The potential predictors of the maximum clear-water scour were compared with the experimental data.

II. A REVIEW OF THE STATE-OF-THE-ART

Several reviews (National Cooperative Highway Research Program 1970; Anderson, 1974; Melville, 1975; and Breusers, Nicollet and Shen, 1977) on local scour around bridge piers have appeared in the

literature in the past several years. A brief summary of the current status on this subject matter is presented in this section.

A. The Mechanism of Local Scour. The system of vortices (horseshoe-vortex system, wake-vortex system, and/or the trailing-vortex system) which develop around the pier and the downward component of velocity on the front face of the of the pier, are the basic agents of local scour, as was long ago recognized by various investigators including Posey (1949), Laursen and Toch (1956), Bata (1960), Neill (1964), Roper, Schneider and Shen (1967), and Melville (1975). The variations in the intensity of the horseshoe vortex and in the strength of the down flow, and the interaction between them during the formation of the scour hole were explained by Melville (1975). The horseshoe vortex is initially small and comparatively weak. With the formation of the scour hole, however, the vortex rapidly grows in size and strength as additional fluid attains a downward component and the strength of the down flow increases. As the scour hole enlarges, the circulation associated with the horseshoe vortex due to its expanding cross sectional area increases but at a decreasing rate. The rate of increase is controlled by the quantity of fluid supplied to the vortex via the downflow ahead of the cylinder. This in turn is determined by the discharge of the approach flow.

An equilibrium condition is attained when the depth of scour ahead of the cylinder is just sufficient so that the magnitude of the vertically downward flow can no longer dislodge surface grains at the bed. The equilibrium depth of scour for a particular bed material and under clear water scour conditions thus should be a function of the magnitude of the downward flow ahead of the cylinder, which in turn is primarily a function of the diameter of the cylinder and the magnitude of the approach flow velocity. The flow depth has only an indirect effect on the magnitude of the downflow and hence on the depth of scour. This concept of the scour development for the clear water case should also be applicable for scour with general sediment-transport. Equilibrium in the latter case is achieved when the depth of scour is such that the

time average rate of sediment erosion and removal by the vertically downward flow and the system of vortices is equal to the time average rate of sediment supply to the scour hole.

B. Estimation of Scour Depth. The flow in the vicinity of the pier is so complex that a complete analytical or numerical description of the scour process is not possible at the present time. Accordingly, phenomena involving local scour around bridge piers have been studied most extensively in laboratory experiments, from which severl empirical formulas have been developed to estimate the maximum scour depths around bridge piers. In general, they are based upon a limited range of data and are applicable to conditions similar to those for which they were derived. It is difficult to confirm their adequacy for design purposes due to limited field measurements. Though there are some similarities among the various empirical relations, they differ widely in terms of the hydraulic variables considered to be significant. Most of the scour relations can be expressed in the form of the following general equation

$$\frac{d_s}{b} = A\left(\frac{y}{b}\right)^m (F)^n + B\left(\frac{D}{y}\right)^p \left(\frac{y}{b}\right)^r \qquad (1)$$

in which d_s is the scour depth measured below mean bed elevation, b is the width of the pier projected on a plane normal to undisturbed flow, D is the mean sediment size, A and B are constants, m, m, p and r are exponents, and the remaining symbols have been defined earlier. The values of the constants A and B, and the exponents m, n, p and r depend upon the pier shape, the angle of attack of the flow, and the sediment properties. Equation 1 indicates that the scour depth is a function of four variables; the pier size, the flow depth, the flow velocity, and the sediment size. The values of the constants and exponents in Eq. 1 for circular piers based on the relations proposed by the various investigators are summarized in Table 1. There are other empirical relations which could not be expressed in the form of Eq. 1; these are listed in Table 2.

TABLE 1 - CONSTANTS AND EXPONENTS IN EQ. 1

Group	Investigator	Regime	Approach	A	B	m	n	p	r	Remarks
I	Breusers (1965)	Incipient motion	Rational	1.40	0	0	0	0	0	
	Larras (1963)	Incipient motion	Rational	$1.42 D_b^{-\frac{1}{4}}$	0	0	0	0	0	
II	Blench (1969)	Sediment transport	Regime	1.80	-1	3/4	0	1	0	y = regime depth
	Laursen (1958)	Sediment	Rational	1.11	0	1/2	0	0	0	Transformed and simplified by Melville (1975)
	Laursen & Toch (1956)	Incipient motion	Rational	1.35	0	0.3	0	0	0	Transformed and simplified by Neill (1964)
	Arunachalam (1965)	Sediment transport	Regime	1.95	-1	5/6	0	1	0	y = regime depth
III	Ahmed (1962)	Sediment transport	Regime	3.18K	-1	1	2/3	1	0	K ≅ 1.2
	Shen et al (1969)	Incipient motion	Rational	11.00	0	1	2	0	0	
V	Shen et al (1969)	Incipient motion	Rational	3.40	0	1/3	2/3	0	0	
	Hancu (1971)	Incipient motion	Rational	2.42	0	1/3	2/3	0	0	
	Inglis-Poona (Thomas, 1962)	Incipient motion	Rational	4.05	-1	3/4	1/2	1	0	

TABLE 2 - SCOUR RELATIONS NOT EXPRESSIBLE IN THE FORM OF EQ. 1

Group	Investigator	Regime	Approach	Formula	Remark
III	Chitale (1962)	clear water	Rational	$\frac{d_s}{y} = (-0.51 + 6.65F - 5.49F^2)$	
IV	Inglis Lacey (1949)	sediment transport	Regime	$D_s = 0.946(Q/f)^{1/3}$	D_s = scour depth below water surface Q = discharge in cfs f = Lacey silt factor $= 1.76\sqrt{D_{50}}$
	Knezevic (1960)	clear water	Rational	$d_s = 8.72 \frac{(q - q')^{3/2}}{y^{5/4} g^{3/4}}$	q = vy q' = q for $d_s = 0$
	Bata (1960)	clear water	Rational	$\frac{d_s}{y_o} = 10(F^2 - \frac{3D}{y})$	
V	Maza (1968)	clear water and sediment transport	Rational	$\frac{d_s}{b} = f(F, y/b)$	graphical form
VI	Hancu (1971)	clear water	Rational	$\frac{d_s}{b} = 2.42(\frac{2V}{V_c} - 1)F_c^{2/3}(y/b)^{1/3}$	V_c =threshold velocity $F_c = V_c/\sqrt{gy}$
	Garde (1961)	-	Rational	$\frac{D_s}{y} = 4.0\eta_1\eta_2\eta_3 \frac{1}{\alpha}(F)^n$	$\alpha = (B - b)/B$ B = clear channel with η_1, η_2, η_3 and n are functions of particle drag coefficient, Froude number & Pier shape
	Chabert and Engeldinger (1956)	clear water and sediment transport	Rational	$d_s = f(b, y, V, D)$	graphical form

The scour relations can be classified in several ways. They are grouped into six categories depending upon the number of significant hydraulic parameters in each relation. The only significant parameter is the pier size in Group I; the flow depth and the pier size in Group II; the flow depth and velocity in Group III; the flow depth and velocity, and the sediment size in Group IV; the flow depth and velocity, and the pier size in Group V; all four parameters in Group VI. The scour formulas are divided into three groups based on the flow regimes; (i) clear water, (ii) incipient sediment motion, and (iii) sediment transport regimes. The formulas for the condition of the incipient sediment motion predict the absolute maximum scour which is assumed to occur at flow velocity approximately equal to threshold velocity. The empirical relations are categorized into two classes based on two different approaches; (i) regime and (ii) rational approaches.

A comparison made by Anderson (1974) of the several formulas listed in Tables 1 and 2 showed that the estimates of the relative scour depths differed widely, particularly for the higher values of Froude number and relative depth. The divergence among the curves representing the various scour formulas clearly indicated that most of these equations are applicable only for certain range of flow conditions and should not be extrapolated for flow conditions outside that range.

A summary of the experimental data including the range of parameters used to develop the various scour formulas is given in Table 3. Some general observations which apply to most studies are as follows:

1. Due to the presumption that the maximum scour occurs at a flow velocity nearly equal to the threshold velocity, most studies in sediment transport regime were conducted with velocities slightly higher than the threshold velocity. This remark explains why certain parameters had a limited range in these studies. None of these studies, therefore, considered the effect of bed forms in their analysis. Shen et al (1969), however, suggested that the amplitude of the bed forms should be added to the equilibrium scour depth for design purposes.

TABLE 3 RANGES OF PARAMETERS

Investigator	Model or Field	Regime	Range of Parameters: Channel width w (m)	Pier size b (cm)	Sediment size D_{50} (mm)	Flow velocity V (m/s)	Flow depth y (cm)	Relative depth y/b	Froude number F	Threshold[1] Froude Number F_c	Comments
Bruesers (1965)	Model	Incipient motion	0.95	5.0 11.0	0.2 0.2	0.20-0.40 0.20-0.40	25.0 50.0	5.0 4.5	0.13-0.26 0.09-0.18	0.19 0.14	Experiments were conducted to verify results obtained by Chabert and Engeldinger. Main purpose of investigation was to study scour due to pile groups in sea beds
Knezevic (1960)	Model	clear water	1.00	10.0	0.2* 1.6* 3.0*	0.12-0.22 0.16-0.38 0.23-0.46	6.5-15.0 6.5-15.0 6.5-15.0	0.7-1.5 0.7-1.5 0.7-1.5	0.10-0.27 0.13-0.48 0.21-0.50	0.23-0.31 0.45-0.61 0.61-0.80	Pier was round-nosed rectangular 10cmx60cm placed parallel to the flow. *D_{90} sand sizes furnished in report. D_{50} computed using $\sigma_g = 1.4$
Inglis-Poona (1962)	Model	Incipient motion	-	5.4 10.7 17.3 17.3	0.3 0.3 0.3 1.3	0.18-0.42 0.30-0.38 0.34-0.45 0.42-0.50	11.5-53.0 25.0-41.0 32.0-61.0 25.0-48.0	2.1-9.6 2.3-3.0 1.9-3.5 1.9-2.8	0.17-0.21 0.19 0.17-0.19 0.23-0.27	0.15-0.27 0.17-0.20 0.14-0.18 0.28-0.36	Piers were round-nosed with a length-to-width ratio of 1.7 and were placed parallel to the flow. In all runs $-0.1<(F-F_c)\leq 0$; tests conducted at four scales; 1/40, 1/65, 1/105, and 1/210
Laursen and Toch (1956)	Model	Incipient motion	1.52	6.1*	0.44 0.58 0.97 1.30 2.25[2]	0.30 0.30-0.61 0.38-0.61 0.46-0.69 0.69-0.76	9.0 6.1-27.4 6.1-24.4 6.1-24.4 9.1-24.4	1.5 1.0-4.5 1.0-4.0 1.0-4.0 1.5-4.0	0.32 0.23-0.64 0.28-0.59 0.44-0.79 0.49-0.72	0.33 0.24-0.42 0.30-0.51 0.36-0.59 0.44-0.63	*Pier was square-nosed dumbell shaped, 6.1cmx40.5cm and set at 30° to the flow. $-0.1<F-F_c\leq 0.15$ for most of runs **Maximum observed scour on the Skunk River for this momentum depth = 213cm
	Field	Sediment movement	41	122	0.45[2]	-	350.**	-	-	-	
Ahmad (1962)	Model	Sediment movement	-	190.5-304.8*	0.24	1.58-3.44	426.7-804.7	2.1-3.6	0.19-0.49	0.05-0.06	Estimates of scour depths are based on river model studies for various bridge sites. *Data is given in prototype dimensions. No model scale given. A scale distortion factor was used to obtain the correct scour depths. Used average discharge per unit width to compute K (defined in Table 2-1) though the flow distributions were largely nonuniform
	Field	Sediment movement	(Maximum scour data on railroad bridge on River Ravi near Lahore, Pakistan from 1948-1958. K values lie between 1.17 and 1.99)								

[1]The values for F_c are based on the threshold velocity determined from the Shields' criterion for the critical shear stress (Vanoni, 1975) and the logarithmic velocity distribution given by $V_c/V_* = 2.5 \ln (11.02yX/D_{50})$, where V_* is the critical shear velocity, and X is a correction factor accounting for the effect of viscosity. A value of 0.01 cm^2/s for the kinematic viscosity of water was assumed in the computations.

[2]Based on the recent data (1979) supplied by USGS

TABLE 3 RANGES OF PARAMETERS (continued)

Investigator	Model or Field	Regime	Range of Parameters: Channel width w (m)	Pier size b (cm)	Sediment size D_{50} (mm)	Flow velocity V (m/s)	Flow depth y (cm)	Relative depth $\frac{y}{b}$	Froude number F	Threshold Froude Number F_c	Comments
Chitale (1962)	Model	clear water	2.44	17.4	0.16	0.24-0.58	16.2-38.1	0.9-2.2	0.13-0.46	0.16-0.22	$-0.20<F-F_c<0.24$. Data show some trends with y/b and D_{50}, but their effects were not considered in the correlation. Some tests at higher velocities had "uncontrolled" sediment movement
					0.24	0.21-0.51	18.3-44.2	1.1-2.5	0.10-0.38	0.15-0.22	
					0.68	0.21-0.53	17.7-44.2	1.0-2.5	0.10-0.40	0.23-0.33	
					1.51	0.27-0.59	15.8-32.9	0.9-3.4	0.15-0.48	0.35-0.46	
Varzeliotis (1960)	Model	Incipient motion	1.12	* 5.0	1.70 1.70	0.48 0.40-0.58	10.7 7.3-15.9	* 1.4-2.1	0.47 0.46	0.54 0.47-0.62	*Experiments covered a range of variables including pier slope, pier length, pier width, angle of attack. Experimental method entailed holding all but one factor constant in each set of runs
Shen et al (1966)	Model	Incipient motion and Sediment transport	1.83	15.2	0.24	0.14-1.02	11.4-26.8	0.8-1.8	0.10-0.95	0.19-0.26	
					0.46	0.38	17.6	1.2	0.29	0.25	
Laursen (1962)	–		–	–	–	–	–	–	–	–	Relationship was based on an analysis of the long contraction solution
Larras (1963)	–		–	–	–	–	–	–	–	–	Equation was primarily based on the experimental results of Chabert and Engeldinger (1956)
Bata (1968)	Model	clear water and Incipient motion	2-2.5	-	0.25	0.34	21.3	-	0.24	0.20	Did not report pier width. Presented results as d_s/y. Piers were models of existing/proposed piers and were constructed in two scales, 1:30 and 1:60
				-	0.50	0.23-0.44	30.0-57.2	-	0.14-0.24	0.17-0.22	
				-	1.50	0.43	42.5	- -	0.21	0.32	
	Field		-	-		1.84-2.28	1740-1880	-	0.15-0.18	-	
Hancu (1971)	Model	clear water and Incipient motion	-	13.0 3.0-20.0 13.0	0.50 2.00 5.00	0.20-0.60 0.28-0.88 0.50-0.90	5.0 5.0-17.5 6.0-16.5	0.4 0.3-2.0 0.5-1.3	0.29-0.86 0.21-0.97 0.44-0.93	0.44 0.46-0.71 0.81-1.11	
Inglis-Lacey (1949)	Field	Sediment movement	–	–	0.17-0.39	–	–	–	–	–	Report on maximum observed scour at 17 bridge sites in India. Most recent observation in 1942. River discharges range from 820 to 63,700 m^3/s

2. Scour depths in all studies, except by Laursen and Toch (1956) who determined scour depths by means of an electric scour meter with flow running conditions, were measured after stopping the flow. Due to the deposition of the suspended sediment in the scour hole during the flow closure, measured scour depths were always less than actual scour depths. The difference between the measured and actual scour depths increases with velocity and becomes significant at velocities higher than threshold velocity. This reasoning explains why Chabert and Engeldinger (1956) did not observe any increase in scour depth with increase in the flow velocity.

3. The scour depth in clear water regime approaches a limit asymptotically and takes a long time to reach this limit for certain flow conditions. It has not been possible to ascertain from the various reports whether limiting depths were attained in all tests. This point should be kept in mind if large scattering in data for this regime is observed.

4. Scour formulas based on 'regime' approach used an empirical formula, derived mainly from canal data, relating the average stable channel depth of an alluvial channel to the dominant discharge and bed material. Some scour formula assumed that scour depths at structures could be expressed as some multiple of the average regime depth. These equations should be applied in cases in which the flow, sediment transport, and channel characteristics are quite similar to those from which the particular formula was derived. The equations based on 'regime' approach are, therefore, not considered in the comparative analysis, which is described later.

5. From the experimental results it may be concluded that the scour depth increases with the pier size. The scour formulas in Groups III & IV in Tables 1 and 2 predict that the scour depth is independent of the pier size and are, therefore, not applicable outside the range of variables from which they are derived. These formulas also are excluded from the comparative analysis.

A comparative analysis of the various predictors for the maximum clear-water scour (incipient sediment motion) which are based on the rational approach and belong to Groups I, II, V and VI is included in Chapter IV. The formulas by Maza (1968), Garde (1961), and Chabert and Engeldinger (1956) are not included in the analysis as they are expressed in the graphical form.

III. EXPERIMENTAL EQUIPMENT & PROCEDURE

A. Equipment. This section briefly describes the flume, the bed material and other instruments used in carrying out the experiments.

Flume: The experiments were conducted in the glass-walled tilting sediment flume located in the West Annex of the Iowa Institute of Hydraulic Research. The working section of the flume is rectangular in cross-section, 27 meters long, 91 centimeters wide, and 46 centimeters deep. Water and sediment are recirculated by two axial-flow, variable-speed pumps, each pump discharging into separate 20-centimeter return lines. Flume discharge is measured by a calibrated orifice meter in each line; the combined maximum discharge is about 160 liters per second. Piezometers for measuring local water surface elevations are located at three-meter intervals along the flume. They are all connected to a central manometer board for ease in determining the slope of the water surface. The slope of the flume can be changed while it is operating by means of an electrically driven tilting mechanism. 25-millimeter diameter rails supported by the flume walls serve as the vertical reference for all elevation measurements.

A motorized instrument carriage rides on the flume rails (Figure 1) along the full length of the channel. The carriage drive is a DC electric motor remotely operated by a solid-state motor control which can be set at any speed in either direction. Instruments attached to the carriage can be positioned anywhere across the width of the flume. A standard point gage with a vertical resolution of 0.3 millimeter is used to measure elevations.

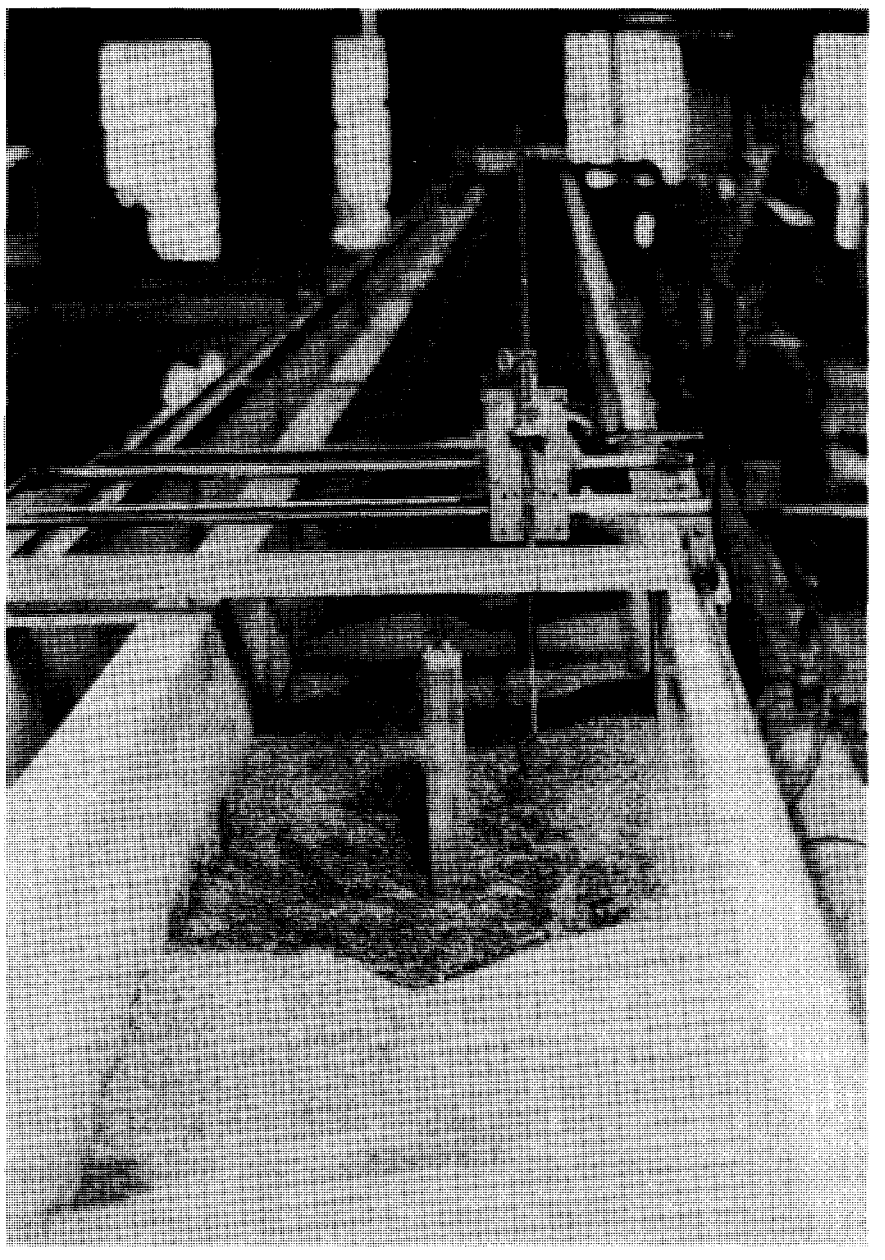

Figure 1. Instrument carriage and flume.

Ultrasonic distance meter: Bed profiles, from which average bed slopes with respect to the flume rails were determined, were measured by means of an ultrasonic distance meter ("sonic sounder"), Model 1054, manufactured by Automation Industries, Inc., Boulder, Colorado, and modified by the Institute. The sensing head of the meter is mounted on the carriage, and as it moves along the channel at constant speed, output (local bed elevations) in the form of voltage levels at specified intervals is recorded on-line via an analog-to-digital converter by the Institute's IBM 1801 Data Acquisition and Control System. Calibration tests of the sonic sounder show a virtually linear relation between voltage level and bed elevation in the range of depths encountered in the project.

Bed material: Three sizes of sand were used as bed material. The fine sand was laboratory grade white quartz and the medium and coarse sands were locally obtained filter sands. Sieve analyses were conducted after recommendations by Vanoni, et al (1961). The particle size distribution for each sand is shown in Figure 2. The respective geometric mean sizes and standard deviations are given below.

Sand	Fine	Medium	Coarse
D (mm)	0.25	1.50	2.50
σ_g	1.34	1.25	1.25

The nominal depth of the sand bed in the flume was about 20 centimeters.

Piers: Two piers, 50.8 millimeters and 101.6 millimeters[1] in diameter, were made from clear plastic tubes. Each pier was built so that the top portion could be removed during data acquisition with the sonic sounder. Both piers were placed in the flume for each run, the smaller pier about 11 meters downstream of the head of the flume and the other pier 9 meters further downstream. The experimental data on the mean velocity distribution downstream of a cylinder of diameter b (Rouse, 1959) show that the maximum velocity difference in the wake of the cylinder

---

[1] All experimental measurements were carried out in FPS system and later converted to SI system.

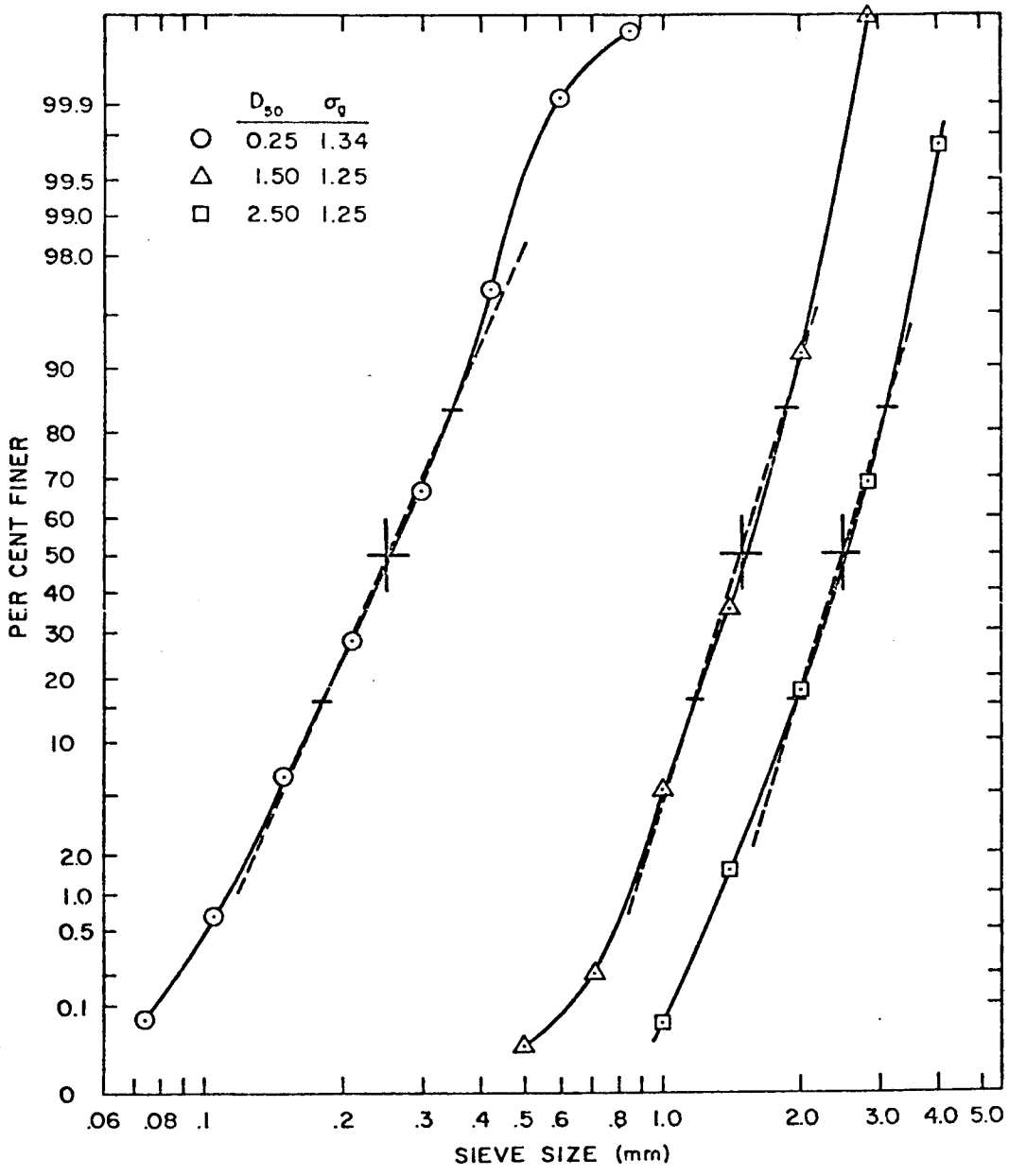

Figure 2. Size frequency graph for three sands.

reduces to less than 1% of the ambient velocity beyond about 170 b downstream of the cylinder. There was, therefore, no significant effect of the upstream pier on the mean velocity distribution of the flow approaching the downstream pier. The effect on the turbulent velocity profile was assumed to be unimportant as the turbulence level in the ambient flow was high.

B. Experimental Procedure

Flow establishment. The depth of flow for all runs was maintained at 10.16 centimeters, except for the depth tests. Uniform flow conditions with the piers in place were established for each run by setting the discharge and then tilting the flume until the bed and water surface slopes were parallel to the flume rails. Exactly parallel conditions were not sought as sonic sounder measurements of the bed profile enabled determination of the bed slope with respect to the flume rails. The total bed slope was the sum of the flume slope and the measured bed slope. The flow was allowed to run until there were no appreciable changes in flow conditions. Once uniform flow was established, the flow was stopped, the flume drained, and the bed around each pier prepared for measuring scour (described below). The flume was then filled again and the run made under the established uniform flow conditions. Each experiment in sediment transport regime was allowed to run long enough for several complete cycles of bed configurations to pass the piers; in clear water regime, it was allowed to run until the approximate maximum scour was reached.

Water surface slope: The water surface slope for each run was determined from the piezometer readings obtained from the manometer board. At higher Froude numbers where the readings fluctuated extensively, the minimum and maximum fluctuations at each station were noted and the averages used in computing the slope. A linear regression program for hand held calculators was used to determine the best fit line on the data.

Mean bed elevation (MBE): After each scour run, the bed profile along the centerline of the flume was measured with the sonic sounder. The

length of a profile was about 14 meters. A marker was placed at either end of the 14-meter interval so that the sonic sounder recorded their presence as discontinuities in the bed profile. The carriage speed was then adjusted so that, at a sampling time interval of 80 milliseconds, approximately 2000 points were collected between the markers. A linear regression analysis was performed on them to determine the bed slope and the MBE at each pier. This analysis was done on the IBM 360 Computer at The University of Iowa Computer Center after transferring the data on cards. As a visual check on the bed profiles, computer-drawn plots of the data were created by the Versatec Plotter facilities available at the Computer Center.

Scour measurement: During the initial phase of the project, it became apparent that the conventional method (stop the flow and measure scour by a point gage) did not yield the correct scour depths around the piers because the scoured holes partially filled in as the flow stopped. The ultrasonic sounder could not be used to measure scour depths without stopping the flow since the faint echoes from the suspended sediment obscured echoes from the sand bed. Since maximum scour was the principal concern, a means of recording it was devised by vertically embedding in the sand strings of yarn spaced at 3.05 centimeters in a square grid pattern around each pier. As the sand was eroded, the exposed portions of the strings bent over at the bed and were covered during the bed aggradation thus preserving the lowest level of scour. Upon completion of each run the strings were excavated (Figure 3) and the points of articulation measured with the point gage. The bed preparation mentioned previously therefore consisted of embedding the strings around the piers after uniform flow conditions were achieved. The maximum scour value for each run was the difference between the MBE (as determined above) and the lowest measured point of scour.

Depth tests: For the depth tests, the flume width was reduced to 61 centimeters by means of a temporary partition and a third pump with a 15 centimeter return line was installed to increase the discharge to about 185 liters per second. The additional pump siphoned water from the downstream end of the flume and discharged it back upstream into the

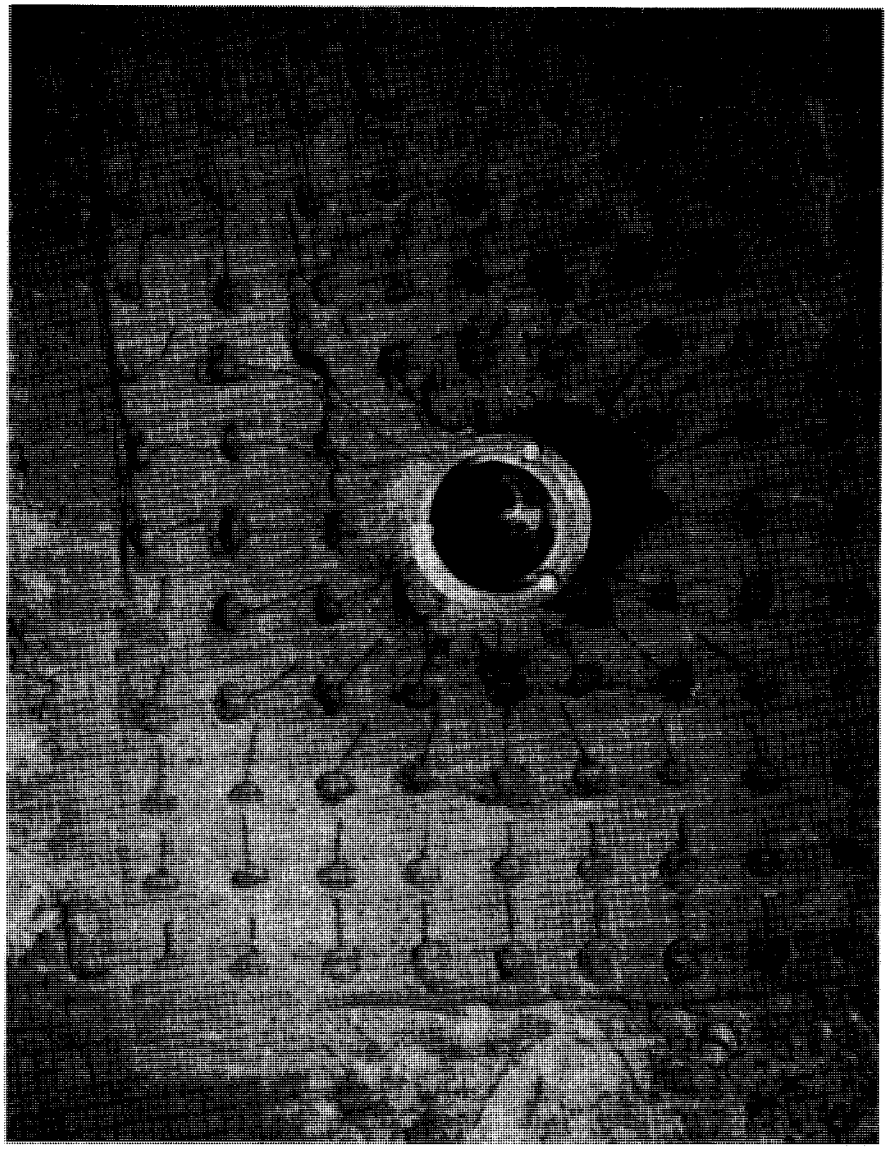

Figure 3. Photograph showing excavated strings.

flume through a diffuser box. Only the smaller pier was used in these tests. The procedures for establishing uniform flow and measuring scour were the same as before. The approximate flow depth for the depth tests was 23 centimeters. One test at low Froude number was conducted with the original flume width to study the effect of the aspect ratio.

IV. EXPERIMENTAL RESULTS

A. Test Parameters. The flow conditions for the various runs and the principal results obtained in these tests are summarized in Table 4. The threshold velocity used in computing threshold Froude number given in column 6 of Table 4 is based on the logarithmic velocity distribution (see Table 3 for the expression) and the Shields' criterion for the critical shear stress. The maximum scour below the mean bed elevation due to bed forms only listed in column 8 is the average of the scour readings measured at the embedded strings located 6 pier diameters (the most upstream row) upstream of the smaller pier. It is assumed that the scour hole around the pier did not affect the scour due to bed forms this far upstream of the pier. The examination of the longitudinal cross-sections of the scour holes confirmed the validity of this assumption. The scour depths presented in columns 9 and 10 are the maximum values below the mean bed elevation observed near the upstream end of the piers, and include the effect of bed forms. Runs No. C-6 and C-7 were conducted with reduced flume width of 61 cm. The flows at Froude number 1.2 and higher in the flume were very rough (Figure 4). The flow conditions particularly in Runs F-4 and M-7 were unsteady and the results for this run are, therefore, questionable. The bed-form conditions for the various runs are given in column 13. No flat-bed regime was observed in the tests with the medium and coarse sands.

B. Shape of the Scour Hole. The data on measured scour depths around each pier were punched on cards, and the longitudinal cross-section

TABLE 1 - SUMMARY OF TEST PARAMETERS AND MODEL RESULTS

Run No.	Sediment Size D_{50} (mm)	Depth y (cm)	Mean Velocity $\bar{v}$ (m/s)	Froude Number F	Threshold Froude Number F_c	Slope S_{-4} x10	Max Scour due to Bed-forms (cm)	Max. Total Scour d_s (cm)		$\frac{d_s}{b}$		Bed Condition
								b=5.08cm (y/b=2)*	b=10.16cm (y/b=1)	b=5.08cm (y/b=2)*	b=10.16cm (y/b=1)	
(1)	(2)	(3)	(4)	(5)	(6)	(7)	(8)	(9)	(10)	(11)	(12)	(13)
F-1	0.25	10.2	0.50	0.50	0.29	20	0.9	8.4	12.0	1.65	1.18	Dunes
F-2			0.75	0.75		22	0.3	9.9	15.0	1.95	1.48	Flat
F-3			1.00	1.00		39	2.1	11.4	15.9	2.24	1.56	Antidune
F-4			1.20	1.20		63	3.4	15.7	18.5	3.09	1.82	Chutes & Pools
M-1	1.50		0.50	0.50	0.50	12	0	8.6	13.2	1.69	1.30	Incipient Motion
M-2			0.65	0.65		35	2.7	8.7	12.3	1.71	1.21	Dunes
M-3			0.75	0.75		51	3.0	8.6	12.4	1.69	1.22	Dunes
M-4			0.85	0.85		73	4.9	9.8	13.9	1.93	1.37	Dunes
M-5			1.00	1.00		112	6.7	11.5	15.4	2.26	1.52	Antidunes
M-6			1.20	1.20		137	6.7	12.9	17.4	2.54	1.71	Antidunes
M-7			1.50	1.50		160	6.4	15.0	-	2.95	-	Chutes & Pools
C-1	2.50		0.50	0.50	0.63	13	∿0	9.7	16.0	1.91	1.57	Flat
C-2			0.62	0.62		19	0	7.3	14.1	1.44	1.39	Incipient Motion
C-3			0.75	0.75		40	2.4	7.5	13.9	1.48	1.37	Dunes
C-4			1.00	1.00		113	3.4	10.3	14.9	2.03	1.47	Dunes
C-5			1.20	1.20		169	5.8	10.7	15.9	2.11	1.56	Dunes
C-6		24.7	0.82	0.53	0.46	10	1.8	8.7(y/b=4.9)	-	1.71(y/b=4.9)	-	Dunes
C-7		21.6	1.41	0.96	0.48	65	5.2	11.3(y/b=4.3)	-	2.22(y/b=4.3)	-	Dunes
C-8		24.1	0.79	0.51	0.47	10	1.8	9.4(y/b=4.7)	-	1.85(y/b=4.7)	-	Dunes

* unless indicated otherwise

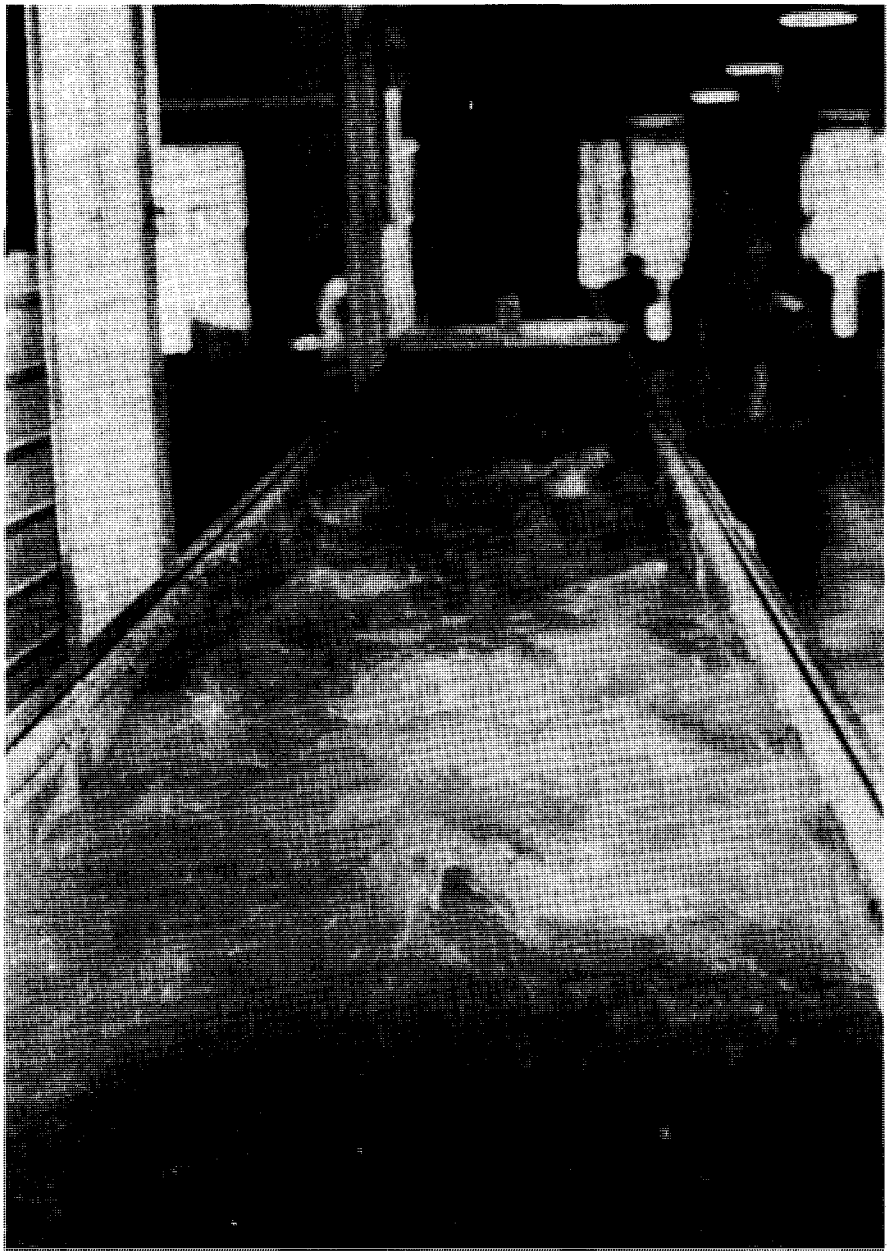

Figure 4. Top view looking upstream showing surface waves. Run F-4.

through the center of the pier and the contours of the scour hole were drawn using the Versatec Plotter. A typical plot for Run C-3 is shown in Figure 5. The plots for other runs are given in Appendix. The data in these figures is shown in thousandths of a foot. The strings were embedded only along the center-line in Runs F-1, M-2, M-4, and C-2; contour plots for these runs are, therefore, not included in the Appendix. The scour holes were similar to a frustum of an inverted cone, and the maximum scour depth always occurred at the upstream end of the pier. Similar observations were recorded by the earlier investigators.

C. Dimensional Analysis. Depth of scour, d_s, can be expressed as a function of the independent variables:

$$d_s = \text{fnc}(\phi, b, \ell, y, U, \rho, \nu, D, \sigma_g, \rho_s, g, t) \qquad (2)$$

where ϕ = pier shape factor, b = pier width perpendicular to the approach flow, ℓ = pier length parallel to the approach flow, y = depth of approach flow, U = velocity of approach flow, ρ = fluid density, ν = fluid kinematic viscosity, D = mean sediment diameter, σ_g = geometric distribution of sediment diameters about the mean, ρ_s = sediment density, g = gravitational acceleration, and t = time. It can be argued that ρ_s of itself is not as significant as is its submerged weight, $\gamma_s' = g(\rho_s - \rho)$, which gives a measure of the buoyancy forces acting on a particle. Substituting γ_s' for ρ_s, Eq. 2 can be nondimensionalized as

$$\frac{d_s}{b} = \text{fnc}\left(\phi, \frac{\ell}{b}, \frac{y}{b}, \frac{Ub}{\nu}, \sigma_g, \frac{\rho U^2}{\gamma_s' D}, \frac{U}{\sqrt{gy}}, \frac{Ut}{b}\right) \qquad (3)$$

where $\frac{\rho U^2}{\gamma_s' D}$ is a variation of Shields' parameter for the beginning of bed movement, with the shear velocity replaced by the mean stream velocity. Some of the terms in Eq. 3 can be eliminated. ϕ and ℓ/b are constants in this study as the piers are circular. The effect of viscosity is considered negligible in the scour process so that Ub/ν can be dropped. σ_g is approximately constant for the three sands with values ranging only

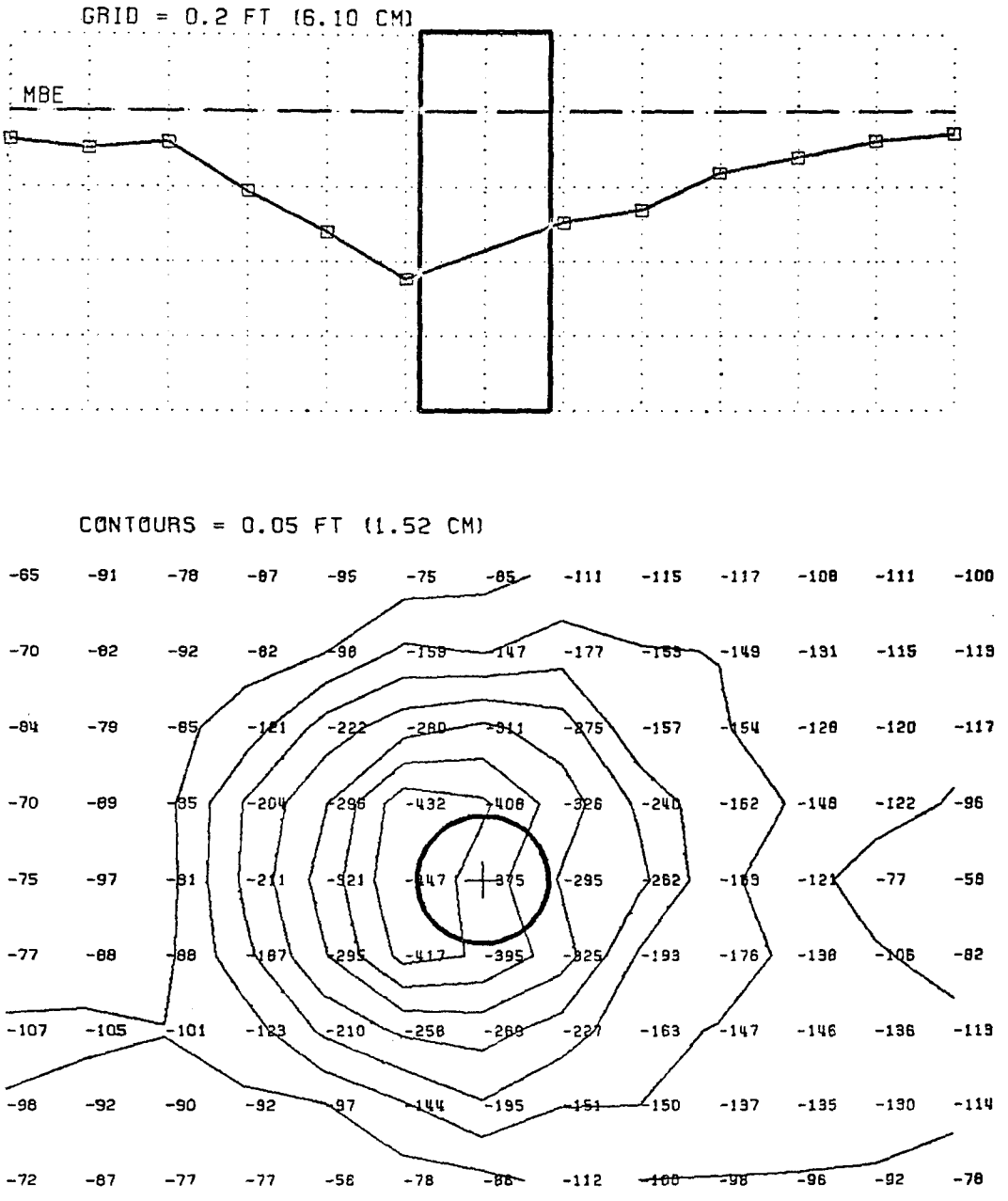

Figure 5. Longitudinal cross section and contours of the scour hole. Run C-3.

from 1.25 to 1.34. And Ut/b is not relevant as time development of scour was not of interest in this study. Thus Eq. 3 can be reduced to

$$\frac{d_s}{b} = \text{fnc}\left(\frac{Y}{b}, \frac{D}{y}, \frac{\rho U^2}{\gamma_s' D}, \frac{U}{\sqrt{gy}}\right) \tag{4}$$

The particular form of $U/\sqrt{gy} = F$, the Froude number of the approach flow, is chosen because of the possible effects of surface waves on scour at high flow velocities. If further analysis is limited to sand in water, then ρ and $\rho_s - \rho$ are constants and the term $\frac{\rho U^2}{\gamma_s' D}$ is in effect a Froude number with D as the characteristic length: $F_d = U/\sqrt{gD}$. Hereinafter, F_d is referred to as the particle Foude number. For a given flow velocity, flow depth and particle size, F and F_d differ only by a constant, indicating that one of the terms is redundant. Furthermore, the relative sediment size, $\frac{D}{y}$ can be expressed as a function of $F_c = \frac{U_c}{\sqrt{gy}}$ or $F_{dc} = \frac{U_c}{\sqrt{gD}}$ using Shields' criterion for the initiation of sediment movement and the logarithmic velocity distribution, where U_c is the critical velocity for the initiation of sediment movement. Thus Eq. 4 can be written as either

$$\frac{d_s}{b} = \text{fnc}\left(\frac{Y}{b}, F_c, F\right) \tag{5a}$$

or

$$\frac{d_s}{b} = \text{fnc}\left(\frac{Y}{b}, F_{dc}, F_d\right) \tag{5b}$$

D. Data Analysis. In the light of the dimensional analysis and the choice of the Froude number as an independent variable, the variations of relative scour depth are plotted in Figs. 6 and 7. The plots in Fig. 6 are based on the Froude number, F, and the plots in Fig. 7 are based on the particle Froude number, F_d. The critical Froude number and the critical particle Froude number for incipient sediment motion, F_c and F_{dc} respectively, are indicated for each of the sand sizes. The scour depth first decreases

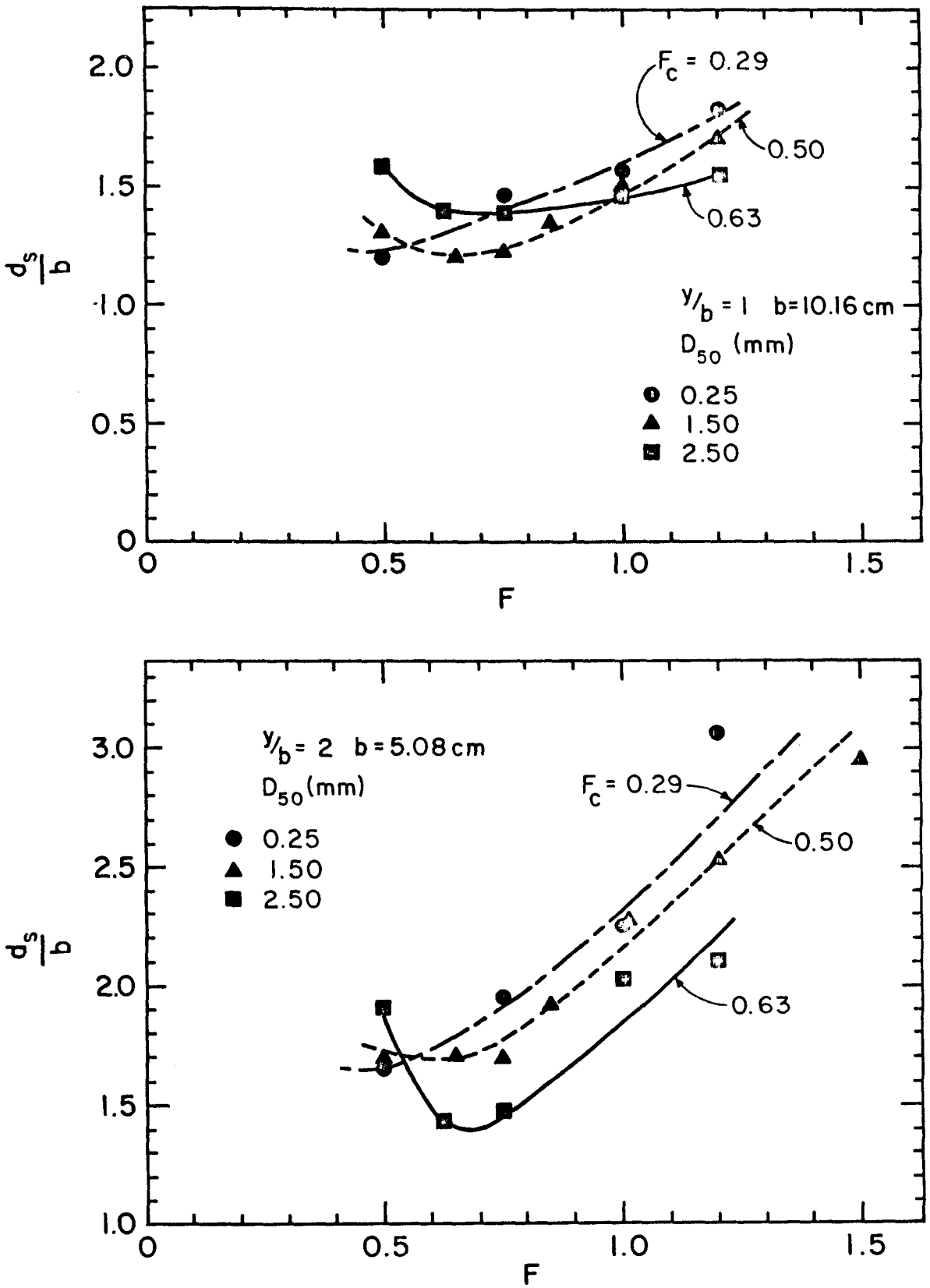

Figure 6. Variation of relative scour with Froude number.

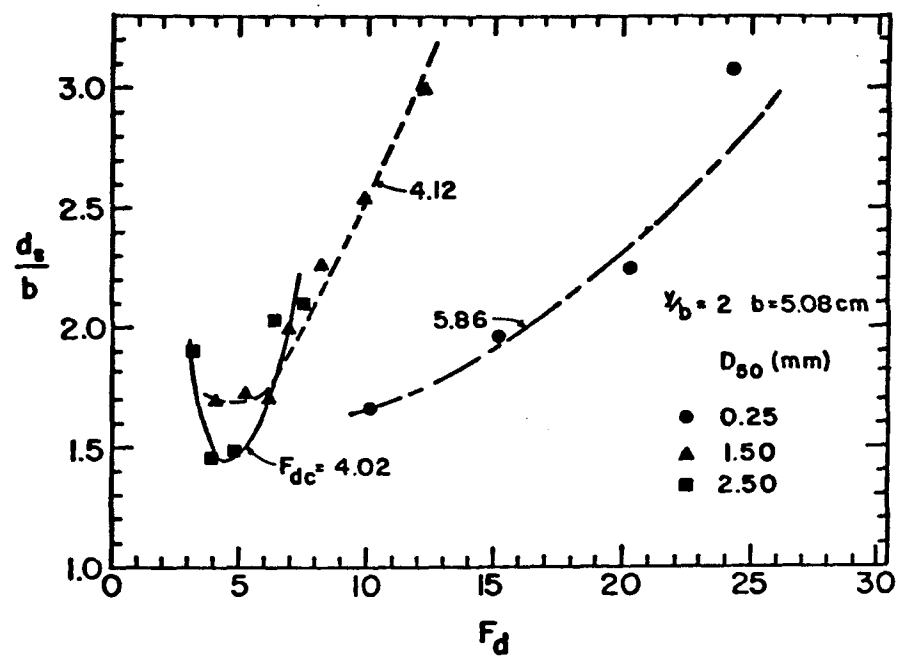

(a)

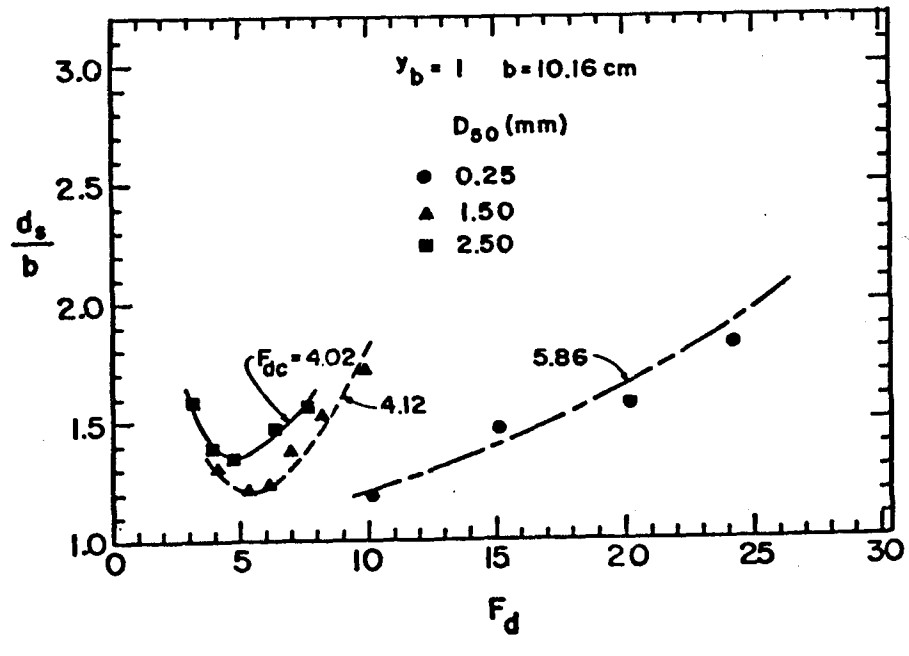

(b)

Figure 7. Variation of relative scour depth with particle Froude number.

and then increases, with increasing Froude number (or velocity). This can be explained in the following way. Maximum clear water scour is that condition where the scour mechanism can no longer dislodge particles near the base of the pier when the stream is flowing at incipient sediment motion conditions. If the stream velocity is increased, the strength of the scour mechanism increases, but now sediment is also transported into the scour hole. If the sediment transport rate into the hole is greater than the corresponding increase in sediment removal rate by the scour mechanism, the net result is a decrease in scour depth, whereupon the new maximum scour depth is marked by the equilibrium between sediment transport rate into the hole and the sediment removal rate by the scour mechanism. As the stream velocity is further increased, the strength of the scour mechanism continues to increase, as does the sediment transport rate. However, the scour mechanism strength increases more quickly with the result that the equilibrium between sediment transport rate into the scour hole and sediment removal rate by the scour mechanism is characterized by a greater scour depth. This reduction in the scour depth at velocities slightly higher than the critical velocity was reported by previous investigators. The increase in the scour depth with Froude number (or velocity) for $(F - F_c) > 0.15$ is, however, not in accord with their conclusion. The reason for this discrepancy possibly lies in the scour measuring techniques.

A comparison of the total scour depth (columns 9 and 10 of Table 4) with the maximum scour due to bed-forms alone (column 8) shows that the contribution of the latter to the former in most cases becomes significant as the velocity increases. However, it should not be concluded that the increase in the scour depth is primarily due to bed-forms; the total scour depth in Run F-2 is higher than that in Run F-1 but the scour depth due to bed-forms alone has the opposite trends. It is neither possible to separate the two components of the scour depth (one due to bed-forms and the other due to the pier) nor necessary as the total scour depth is required in designing a pier. Hence, the formula to predict the total scour depth will be developed.

The scour around the pier reaches equilibrium when the time average rate of sediment erosion and removal by the vertically downward

flow along the face of the pier and the system of vortices around the pier is equal to the time average rate of sediment supply to the scour hole. The latter, according to Onishi, Jain and Kennedy (1976), is proportional to $(F - F_c)^n$. This observation suggests that F and F_c in Eq. 5a or F_d and F_{dc} in Eq. 5b can be grouped as $(F - F_c)$ or $(F_d - F_{dc})$, respectively. If the data points corresponding to each of the curves in Figures 6 and 7 are selected so that (i) $F > F_c$ or $F_d > F_{dc}$, and (ii) only those consecutive points which increase monotonically are chosen, then it is possible to fit a curve to the data of the form

$$\frac{d_s}{b} = A_1 \left(\frac{y}{b}\right)^{\alpha_1} (F - F_c)^{\beta_1} \tag{6a}$$

or

$$\frac{d_s}{b} = A_2 \left(\frac{y}{b}\right)^{\alpha_2} (F_d - F_{dc})^{\beta_2} \tag{6b}$$

where A_1, α_1, β_1 and A_2, α_2, β_2 are constants to be determined from the data. A multiple-linear regression analysis of the data yielded $A_1 = 1.86$, $\alpha_1 = 0.49$ and $\beta_1 = 0.26$ with $r^2 = 0.896$; and $A_2 = 1.19$, $\alpha_2 = 0.52$ and $\beta_2 = 0.14$ with $r^2 = 0.746$. (r^2 is a measure of the dependence of d_s/b upon the independent variables operating jointly. $r^2 = 1$ indicates a perfect correlation.) Based upon the r^2 values, the regression analysis shows that Eq. 6a is the preferred form of the functional relationship since Eq. 6a yields a better fit to the data. Rounding values of α_1 and β_1 to the nearest 1/4 and substituting them and the value for A_1 into Eq. 6a, the following predictor equation is obtained:

$$\frac{d_s}{b} = 1.86 \left(\frac{y}{b}\right)^{0.5} (F - F_c)^{0.25} \tag{7}$$

Figure 7 shows that all of the curves increase monotonincally if $F - F_c \geq 0.15$. A plot of the data using Eq. 7 with the restrictions $0.15 \leq (F - F_c) \leq [1.2]$ and $[1] \leq y/b \leq 2$ is given in Fig. 8, with additional data included from studies by Chabert and Engeldinger (1956)

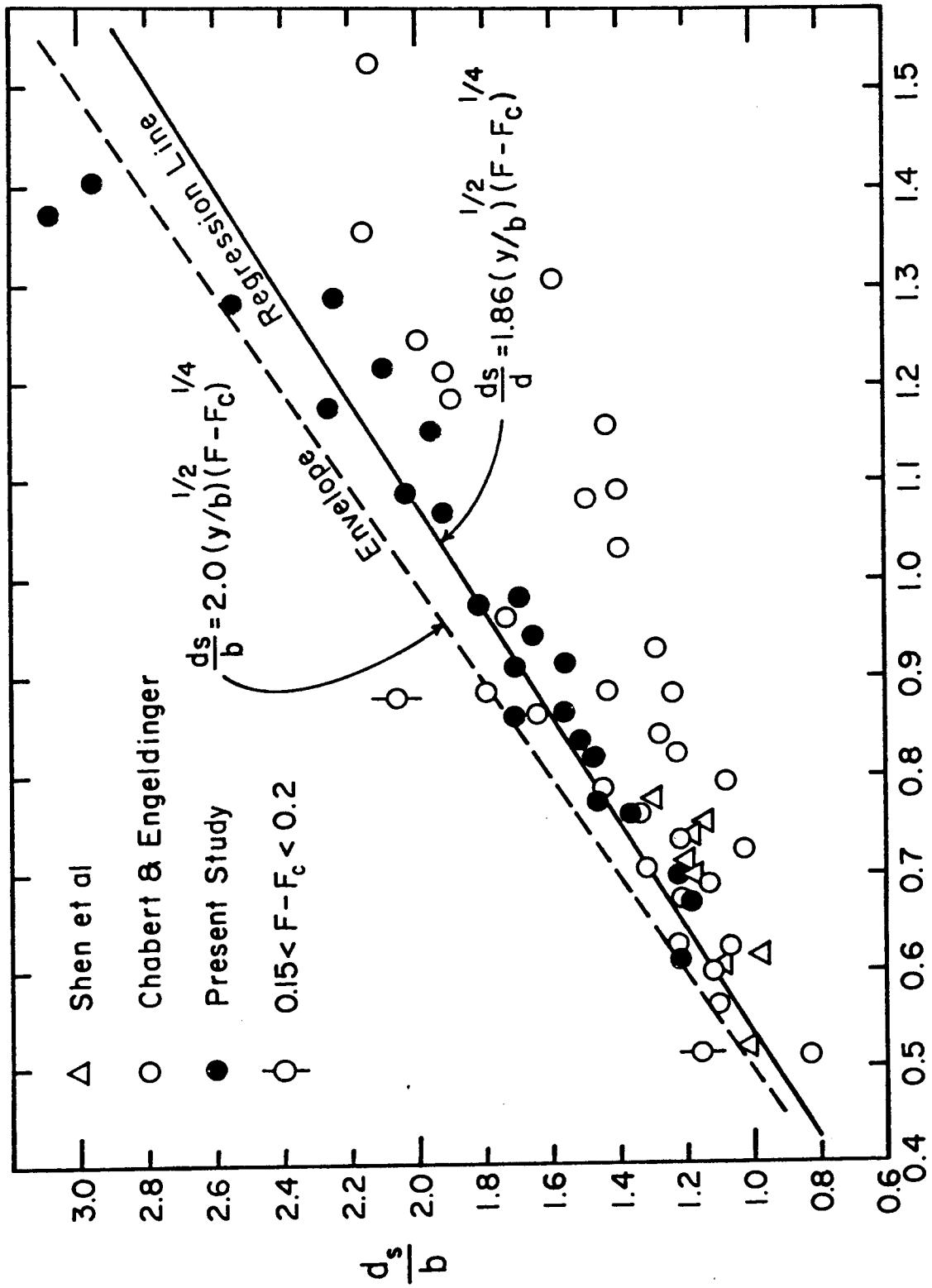

Figure 8. Comparison of Eq. 4-4 with experimental data.

and Shen et al (1969) for comparative purposes. Some of the data points of other investigators, particularly for which the flow velocity was much higher than the threshold velocity, lie below the regression line as the measured scour depth in these tests was less than the actual scour depth due to the deposition of the suspended sediment in the scour hole during the flow closure. Equation 6a with $A_1 = 2.0$ envelopes all the data for $(F - F_c) \geq 0.2$ except for two data points corresponding to Runs F-4 and M-7 in which the flow conditions in the flume were unsteady due to the formation of chutes and pools on the bed. The equation for the envelop is

$$\frac{d_s}{b} = 2.0\left(\frac{y}{b}\right)^{0.5}(F - F_c)^{0.25} \tag{7a}$$

Depth tests: To evaluate the effects on scour of very large relative depths, a few tests (Runs No. C-6, C-7 and C-8) using only smaller piers were conducted at relative depths of about 5. The flow conditions for Runs C-6 and C-8 were almost identical except the flume widhts in the two runs were 61 cm and 91 cm, respectively. The data for Run C-7 were not used in the correlation analysis. The observed scour is about 70% of the scour predicted by Eq. 7. It indicates that Eq. 7, which was developed using data only for y/b = 1 and 2, does not predict scour depths accurately at high relative depths. The observed scour depths in Runs C-6 and C-8 are almose equal. The blockage effects on scour in these tests were, therefore, not significant.

E. Maximum clear-water scour. Equation 5a for $F \cong F_c$ can be simplified to

$$\frac{d_s}{b} = f\left(\frac{y}{b}, F_c\right) \tag{8}$$

The scour formulas of Group V in Tables 1 and 2 are in the form of Eq. 8. This equation would be in accord with the scour formulas of

Group II if the influence of F_c on scour depth is found to be small. If the effect of the depth of flow in addition is found to be insignificant, Eq. 8 would belong to the scour formula of Group I. In order to determine the range of flow parameters for which the various scour formulas are valid, these formulas are compared with the available scour data for circular piers. A summary of the experimental data used in this comparative analysis is presented in Table 5. Only flow conditions with $0.02 < (F - F_c) < 0.1$ were included; the lower limit of 0.02 instead of zero was used to insure that the equilibrium scour depth was achieved in the experiment.

The comparison between the observed scour depths (Table 5) and the scour depth predicted by various formulas is shown in Figure 9. The values of linear correlation coefficient, r, between the observed and predicted scour depth are also included in these figures. The correlation coefficient indicates how well the equation fits the data. The lines of perfect agreement based on formulas by Larras, Shen et al, and Laursen and Toch form an envelope for all data. Breusers' relation envelops the data for $(y/b) \lesssim 3$ only and hence underpredicts scour depths for $(y/b) \gtrsim 3$. The scour formula by Laursen is similar to that by Laursen and Toch as the former was derived by adjusting a constant in the solution for long constriction to agree with the latter. Laursen's relation, however, underpredicts for $y/b \lesssim 1$. The expressions by Shen et al, and Hancu are identical except for the coefficient A (Eq. 1). Hancu's formula with A = 2.42 seems to give the best fit for the data while Shen's formula with A = 3.40 envelops the data. Inglis-Poona's relation is in agreement with data for fine sand ($D \lesssim 0.5$ mm) and $y/b \lesssim 4$.

From design and safety considerations a predictor which envelops the experimental data is desirable. The formulas by Larras, Shen et al, and Larras and Toch fall in this category. An arbitrary criterion, that a formula is satisfactory if it over-predicts less than 30 percent of the observed scour depth, is adopted to compare these three formulas. This criterion is represented by a dashed line in Figure 9. This criterion is met by the formula of Larras for $y/b \gtrsim 3$, Shen et al for fine sand and $y/b \gtrsim 1$, and Laursen and Toch for almost all of the data. It can, therefore, be inferred that the scour formula of Laursen

TABLE 5 - SUMMARY OF DATA USED IN COMPARATIVE ANALYSIS

Flow velocity (m/s)	Pier diameter (cm)	Mean sediment size (mm)	Flow depth (cm)	Max. scour depth (cm)	Investigator
0.82	5.1	2.50	24.7	8.7	Present study
0.40	15.2	0.24	21.9	18.0	Shen et al
0.32	15.2	0.24	11.6	13.4	
0.36	15.2	0.24	15.6	15.8	
0.38	15.2	0.24	20.6	17.1	
0.44	15.2	0.24	21.0	21.0	
0.41	15.2	0.24	26.3	18.6	
0.38	15.2	0.46	17.6	16.6	
0.50	91.4	0.46	61.0	54.9	
0.85	5.0	3.00	20.0	7.0	Chabert &
0.85	10.0	3.00	20.0	12.5	Engeldinger
0.85	15.0	3.00	20.0	18.5	
0.76	5.00	3.00	10.0	8.7	
0.76	10.0	3.00	10.0	13.1	
0.76	15.0	3.00	10.0	17.5	
0.66	5.0	1.50	20.0	9.8	
0.66	10.0	1.50	20.0	17.0	
0.66	15.0	1.50	20.0	20.3	
0.40	5.0	0.52	19.7	9.5	
0.40	10.0	0.52	19.7	12.2	
0.40	15.0	0.52	19.7	14.9	
0.42	5.0	0.52	35.0	9.0	
0.42	10.0	0.52	35.0	12.0	
0.42	15.0	0.52	35.0	13.7	
0.37	10.0	0.52	10.0	11.5	
0.37	15.0	0.52	10.0	13.3	
0.30	13.0	0.50	5.0	11.3	Hancu

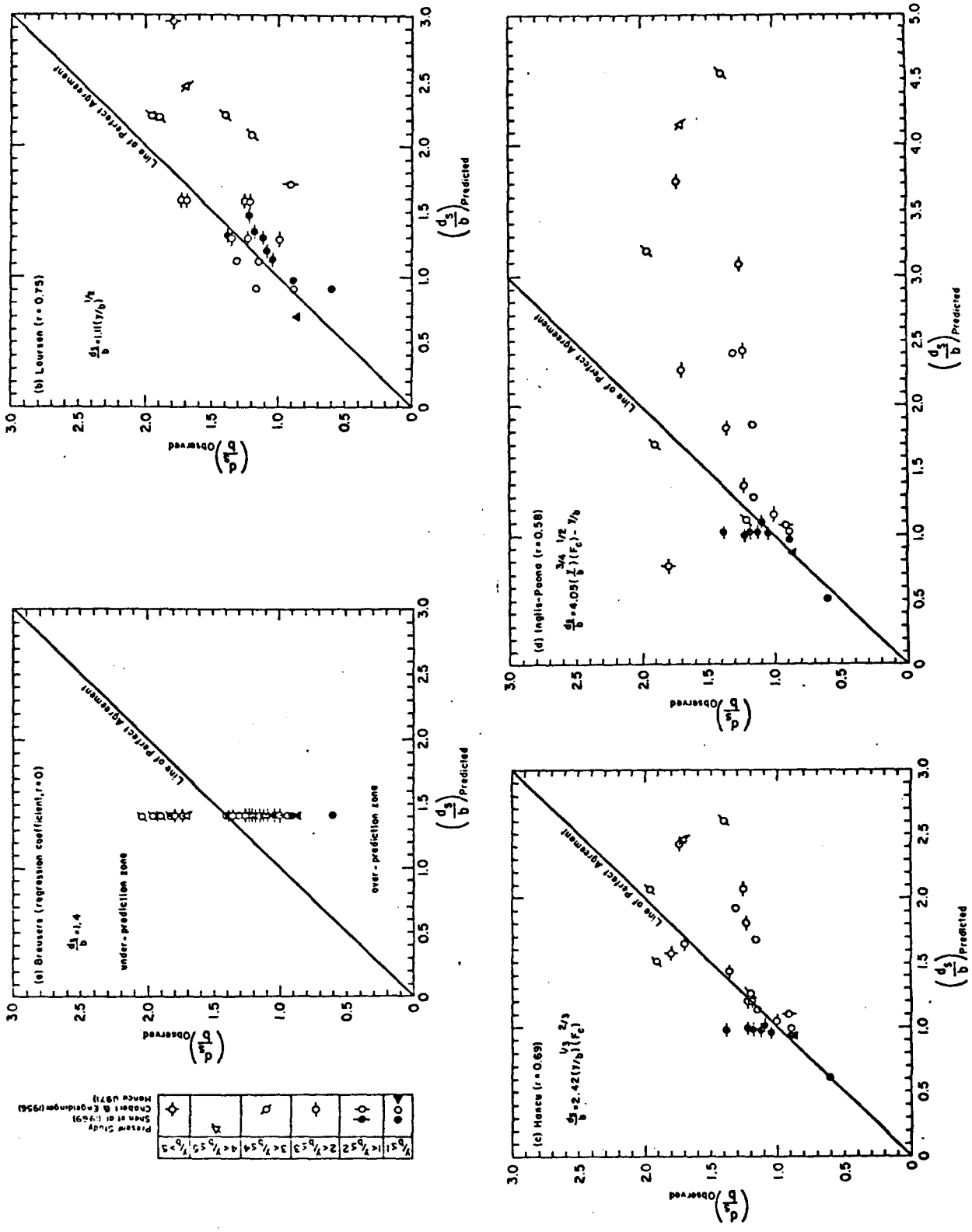

Figure 9. Comparison of various scour formulas with experimental data.

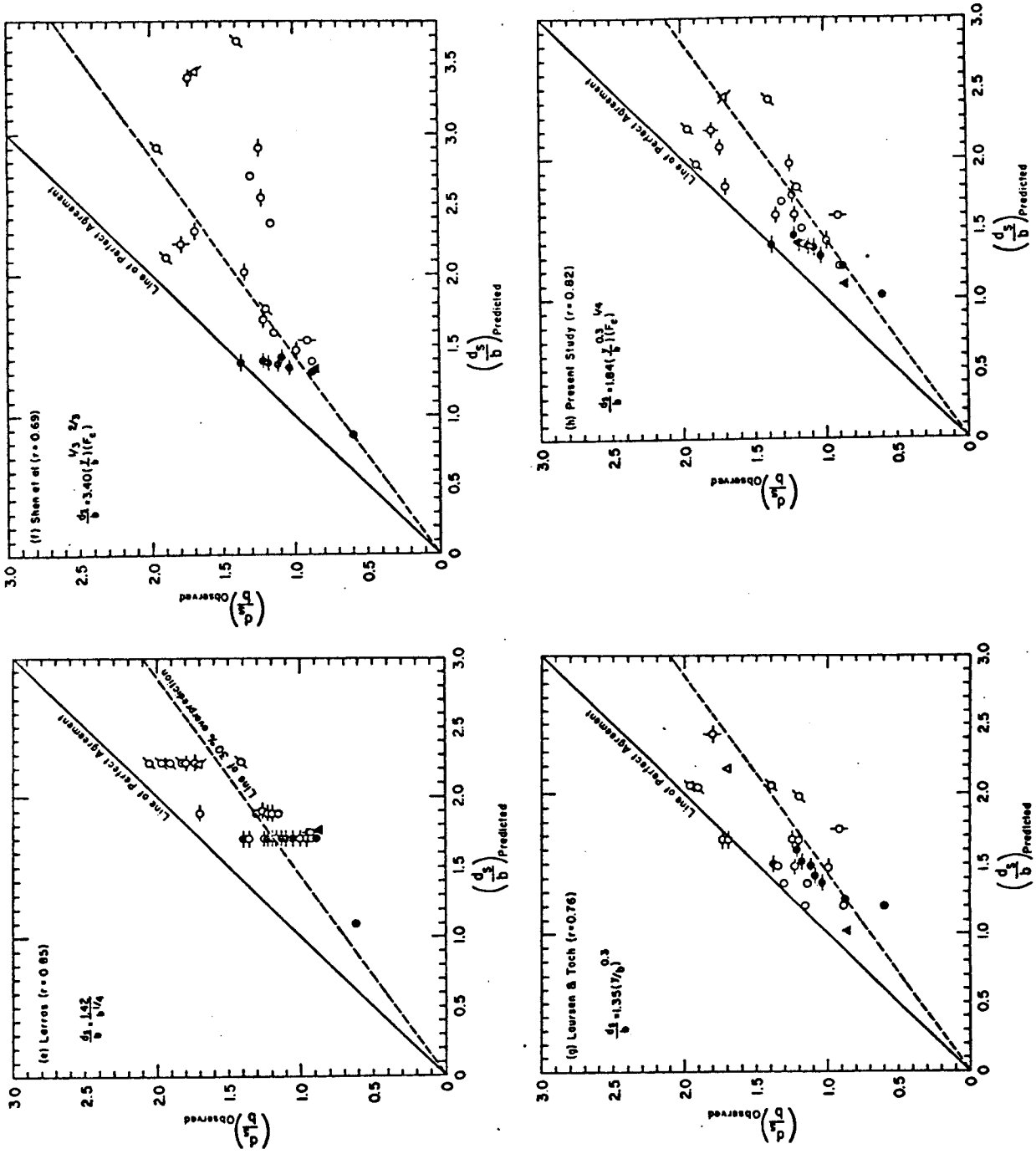

Figure 9. Comparison of various scour formulas with experimental data (continued).

and Toch is the best among these formulas to predict the maximum clear water scour.

A regression analysis of the data (Table 5), based on the assumption that the relative scour depth is a power function of the threshold Froude number and the relative depth, yielded

$$\frac{d_s}{b} = 1.41 \left(\frac{Y}{b}\right)^{0.30} (F_c)^{0.25} \qquad (9)$$

The coefficient 1.41 in Eq. 9 was modified to 1.84 in order to form an envelop for all data; it resulted in

$$\frac{d_s}{b} = 1.84 \left(\frac{Y}{b}\right)^{0.30} (F_c)^{0.25} \qquad (10)$$

The comparison of Eq. 9 and 10 with the data is presented in Figure 9(h). The dashed line in this figure represents the criterion (30 percent over prediction) mentioned before. This equation is satisfactory for almost all of the data as it is the case for Laursen and Toch formula. The exponent of (y/b) in Eq. 10 is identical to that in the Laursen and Toch formula. These two formulas predict the same scour depth for $F_c = 0.29$. Equation 4-7 for $F_c < 0.29$ predicts less scour depths than that given by Laursen and Toch formula. Equation 10 is a better predictor for the maximum clear-water scour than the Laursen and Toch formula due to the following reasons:

1. The laboratory experiments on local scour conducted recently by Ettema (1976), Nicollet (1971) and Hancu (1971) indicate that the maximum clear water scour depends upon the sediment size. Equation 10 also shows that scour depth is a function of sediment size (F_c depends upon the sediment size), while Laursen and Toch equation predicts that it is independent of sediment size.

2. The correlation coefficient for Eq. 10 is higher than that for Laursen and Toch relation.

3. For most practical cases F_c is small and probably less than 0.3; Equation 10 predicts less (hence leading to an economical design) but safe (because it forms the envelop for all data) scour depth.

An attempt to develop a scour formula for clear-water regime ($F < F_c$) proved futile. A lot of scatter in the available experimental data was observed. This scatter was probably due to insufficient time allowance for the equilibrium scour to be attained in most experiments. Furthermore, a scour predictor for $0 \lesssim (F - F_c) \lesssim 0.2$ could not be developed as there are not enough experimental data available in this range of Froude number. The scour depth for this range of Froude number is, however, bounded by the scour depths given by Eq. 7a and Eq. 10. It can be shown that Eq. 7a predicts a greater scour depth than Eq. 10 when the following condition holds,

$$\frac{F}{F_c} \geq 1 + 0.716 \left(\frac{y}{b}\right)^{-0.8} \tag{11}$$

For example, for the relative depth y/b = 1, Eq. 7a should be used to predict the scour depth if $F/F_c > 1.716$.

V. CONCLUSIONS

The scour depth around a circular pier in sediment transport regime ($F > F_c$) first slightly decreases and then increases with the increase in the Froude number. Scour depth at high Froude numbers is larger than the maximum clear-water scour. The contribution of bed-form scour to the total scour depth becomes significant with higher flow velocities. The regression analysis of the experimental data gave the following expression for the total scour depth:

$$\frac{d_s}{b} = 1.86 \, (F - F_c)^{0.25} \left(\frac{y}{b}\right)^{0.5}; \text{ for } F - F_c \geq 0.15 \tag{7a}$$

The regression analysis of some of the experimental data of the previous investigators gave the following expression (Eq. 9) for the maximum clear-water scour depth:

$$\frac{d_s}{b} = 1.41\ (y/b)^{0.3}(F_c)^{0.25} \tag{9}$$

On increasing the coefficients 1.86 to 2.0 in Eq. 7a and 1.41 to 1.84 in Eq. 9, the modified equations envelop the data. The following two equations are, therefore, recommended for design:

$$\frac{d_s}{b} = 2.0(F - F_c)^{0.25}(y/b)^{0.5} \text{ for } (F - F_c) \geq 0.2 \tag{7a}$$

$$\frac{d_s}{b} = 1.84(F_c)^{0.25}(y/b)^{0.3} \text{ for maximum clear-water scour} \tag{10}$$

Eq. 7a predicts a greater scour depth than Eq. 10 and should be used to predict the scour depth when the following condition holds

$$\frac{F}{F_c} \geq 1 + 0.716\left(\frac{y}{b}\right)^{-0.8} \tag{11}$$

It is further suggested that similar experiments at high Froude numbers be conducted to investigate the effect on scour of the pier shape and the large relative depth.

REFERENCES

Ahmed, M., Discussion of "Scour at Bridge Crossings," by E.M. Laursen, Trans. ASCE, Vol. 127, pt. 1, 1962, pp. 198-206.

Anderson, A.G., "Scour at Bridge Waterways - A Review," Rep. No. FHWA-RD-75-89, Federal Highway Administration, Washington, 1974.

Arunachalam, K., "Scour around Bridge Piers," Journal of Indian Roads Congress, Paper No. 251, 1965.

Bata, C., "Erozija oko novosadskog mostovskog stuba," (serbian), (Scour around Bridge Piers), Institut za Vodoprivreder, Jaroslav Cerai Beozrod Yugoslavia, 1960. English translation by Markovic filed at Colorado State University, Fort Collins.

Blench, T., "Mobile Bed Fluviology," University of Alberta Press, Edmonton, Alberta, Canada, 1969.

Breusers, H.N.C., "Scour Around Drilling Platforms," Bulletin, Hydraulic Research 1965, IAHR, Vol. 19, 1965, p. 276.

Breusers, H.N.C., Nicollet, G., and Shen, H.W., "Local Scour Around Cylindrical Piers," Journal of Hydraulic Research, IAHR, Vol. 15, No. 3, 1977, pp. 211-252.

Chabert, J. and Engeldinger, P., "Etude des affouillements autour des piles de ponts," Laboratoire National d'Hydraulique, Chatou, France, 1956.

Chitale, S.V., Discussion of "Scour at Bridge Crossings," by E.M. Laursen, Trans. ASCE, Vol. 217, pt. 1, 1962, pp. 191-196.

Ettema, R., "Influence of Bed Material Gradation on Local Scour," Report No. 124, School of Engineering, Univ. of Auckland, Auckland, New Zealand, 1976.

Garde, R.J., "Local Bed Variation at Bridge Piers in Alluvial Channels," University of Roorke Research Journal, Vol. IV, India, 1961.

Hancu, S., "Sur le Calcul des Affouillements Locaux dans la Zone des Piles du Pont," Proc. 14th Congress, IAHR, Vol. 3, 1971, pp. 299-306.

Inglis, C.C., "The Behaviour and Control of Rivers and Canals," Research Publication No. 13, pt. 2, Central Power, Irrigation and Navigation Report, Poona Research Station, India, 1949.

Knezevic, B., "Prilog proucavanju erozije oko mostoviskih stubova," (Serbian), (Contributions to Research Work of Erosion around Bridge Piers), Institut za Vodeprivredu Jaroslar Ceri Beograd, Yugoslavia, 1960. Translated by Markovic, filed at Colorado State University, Civil Engineering Department, Ft. Collins, Colorado.

Larras, J., "Profondeurs Maximales d'erosion des fonds mobiles autour des piles en rivier," Annales des Ponts et Chausses, Vol. 133, No. 4, 1963, pp. 411-424.

Laursen, E.M., "Scour at Bridge Crossings," Iowa Highway Research Board, Bulletin No. 8, 1958.

Laursen, E.M. and Toch, A., "Scour around Bridge Piers and Abutments," Bulletin No. 4, Iowa Highway Research Board, 1956.

Maza Alvarex, J.A., "Scour in River-Beds," Instituto de Ingenieria, Universidad Nacional Autonoma de Mexico, Ciudad Universitaria, Mexico, 1977.

Melville, B.W., "Local Scour at Bridge Sites," Rep. No. 117, School of Engineering, Univ. of Auckland, Auckland, New Zealand, 1975.

National Cooperative Highway Research Program, "Scour at Bridge Waterways," Synthesis Report No. 5 of Highway Practice, 1970.

Neill, C.R., "Local Scour around Bridge Piers," Highway and Rive eng. Div., Research Council of Alberta, Canada, 1964.

Neill, C.R., "River-bed Scour," A Review for Engineers, Canadian Good Roads Assn; Tech. Publ, No. 23, 1964.

Neill, C.R., Discussion on "Local Scour around Bridge Piers" by When, Schneider and Karaki, Proc. ASCE Journal of Hyd. Div., Vol. 96, HY5, 1970.

Nicollet, G., "Deformation des Lits Alluvionnaires; Affouillements Autour des Piles de Ponts Cylindriques," Laboratoire Nacional d'Hydraulique, Chatou, France, 1971.

Onishi, Y., Jain, S.C., and Kennedy, J.F., "Effects of Meandering in Alluvial Streams," Journal of the Hyd. Div., ASCE, Vol. 102, HY7, 1976.

Posey, C.J., "Why Bridges Fail in Floods," Civil Eng., Vol. 19, 1949, pp. 42-90.

Roper, A.T., Schneider, V.R. and Shen, H.W., "Analytical Approach to Local Scour," Proc. XII Congress of IAHR, Vol. 3, Ft. Collins, 1967, pp. 151-167.

Rouse, H., Advanced Mechanics of Fluids, Wiley, 1959, p. 390.

Shen, H.W., Schneider, V.R. and Karaka, S., "Local Scour around Bridge Piers," Proc. ASCE, Journal of Hydraulics Div., Vol. 95, HY6, 1969.

Thomas, A.R., Discussion of "Scour at Bridge Crossings," by E.M. Laursen, Trans. ASCE, Vol. 127, PE 1, 1962, pp. 196-198.

Vanoni, Vito A et al., "Lecture Notes on Sediment Transportation and Channel Stability," W.M. Keck Laboratory of Hydraulics and Water Resources, California Institute of Technology, Report No. KH-R1, 1961.

Vanoni, Vito A., Sedimentation Engineering, ASCE-Mauals and Reports on Engineering Practice, No. 54, American Society of Civil Engineers, 1975.

Varzeliotis, A.N., "Model Studies of Scour Around Bridge Piers and Stove Aprons," M.S. Thesis, University of Alberta, Canada, 1960.

Longitudinal cross-sections and contours of the scour holes

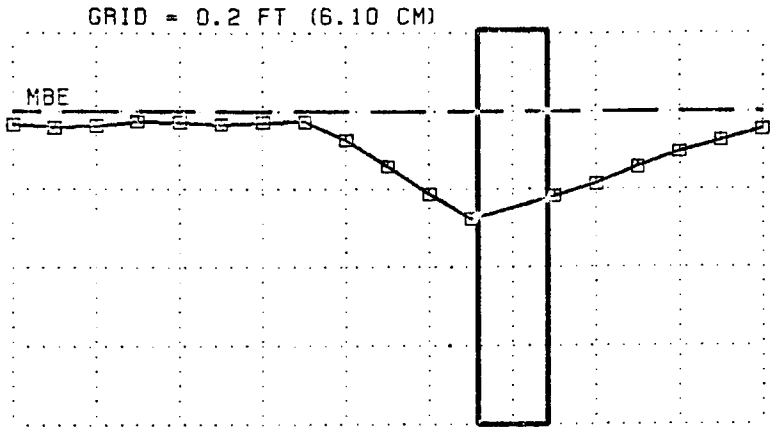

Run F-1 FR=.05 Y/B=2 D50=0.25MM 2-inch pier

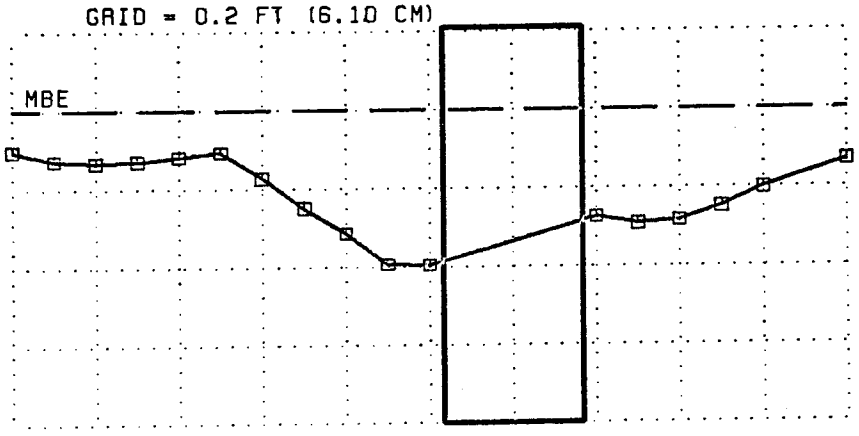

Run F-1 FR=.5 Y/B=1 D50=0.25MM 4-inch pier

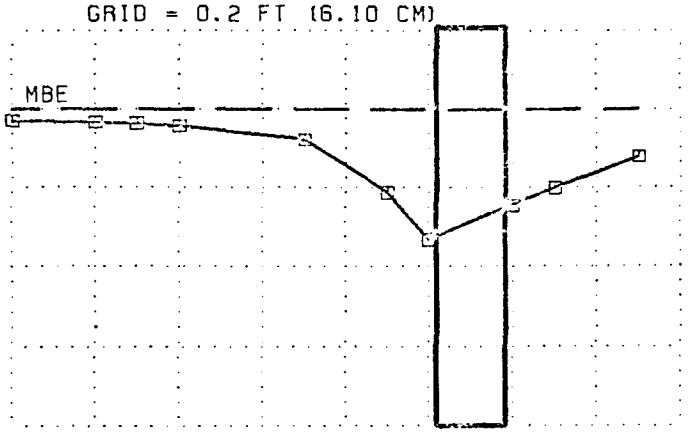

CONTOURS = 0.05 FT (1.52 CM)

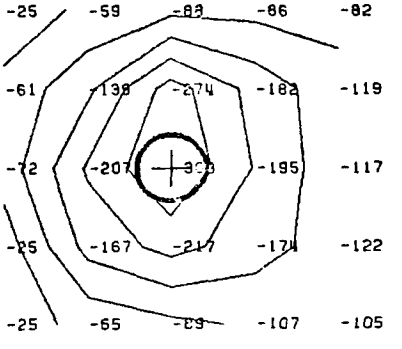

RUN F-2 FR=0.75 Y/B=2 D50=0.25MM 2-INCH PIER

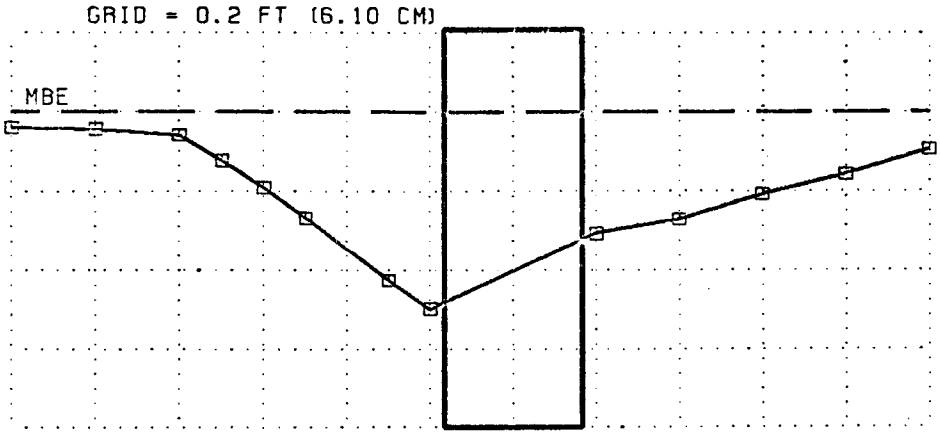

CONTOURS = 0.05 FT (1.52 CM)

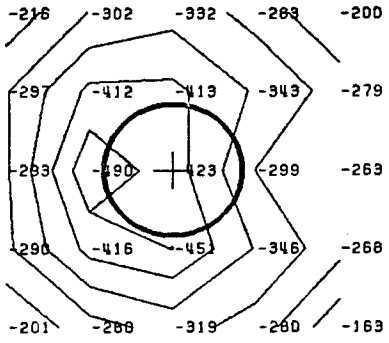

RUN F-2 FR=0.75 Y/B=1 D50=0.25MM 4-INCH PIER

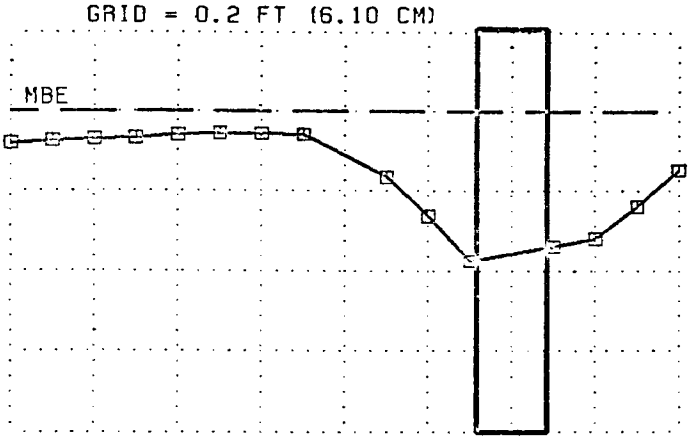

CONTOURS = 0.05 FT (1.52 CM)

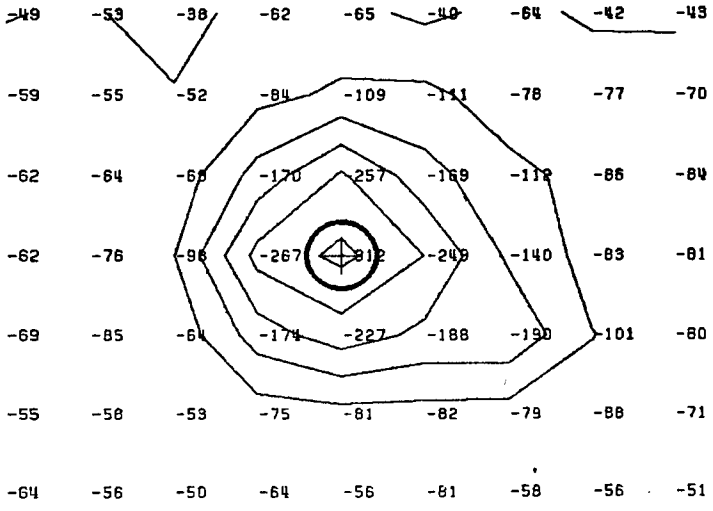

RUN F-3 FR=1.0 Y/B=2 D50=0.25MM 2-INCH PIER

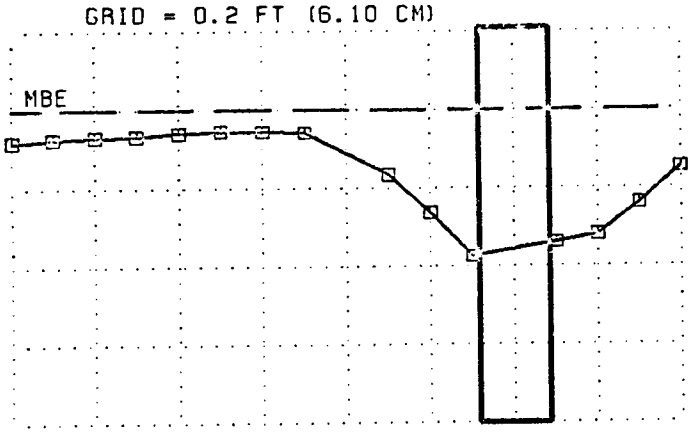

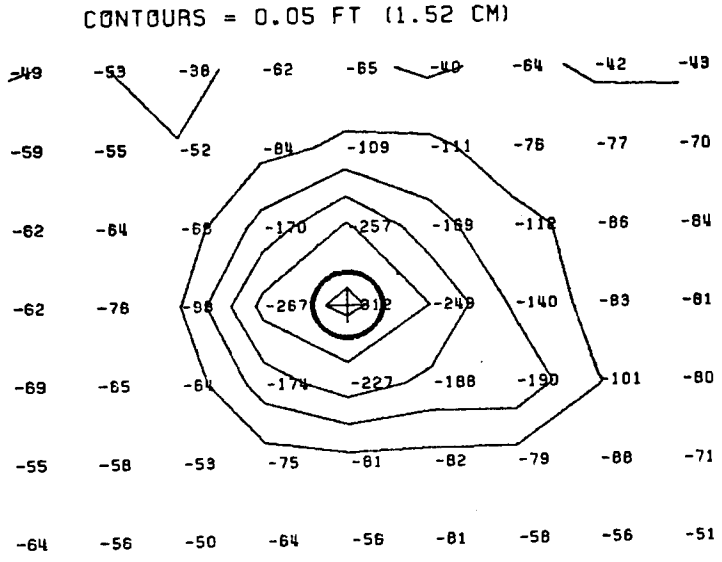

RUN F-3 FR=1.0 Y/B=2 D50=0.25MM 2-INCH PIER

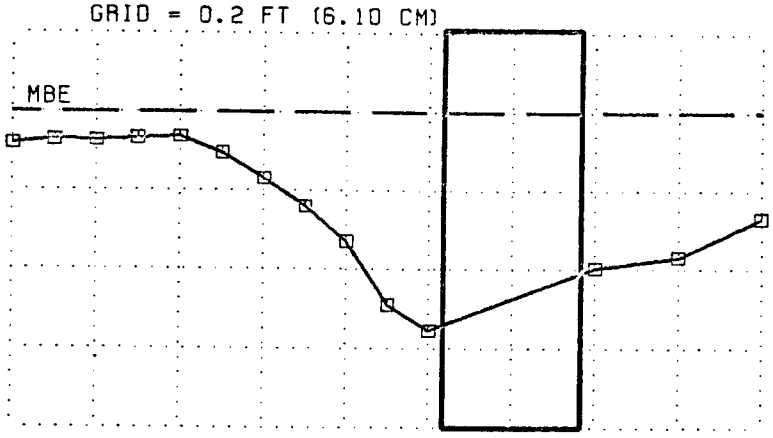

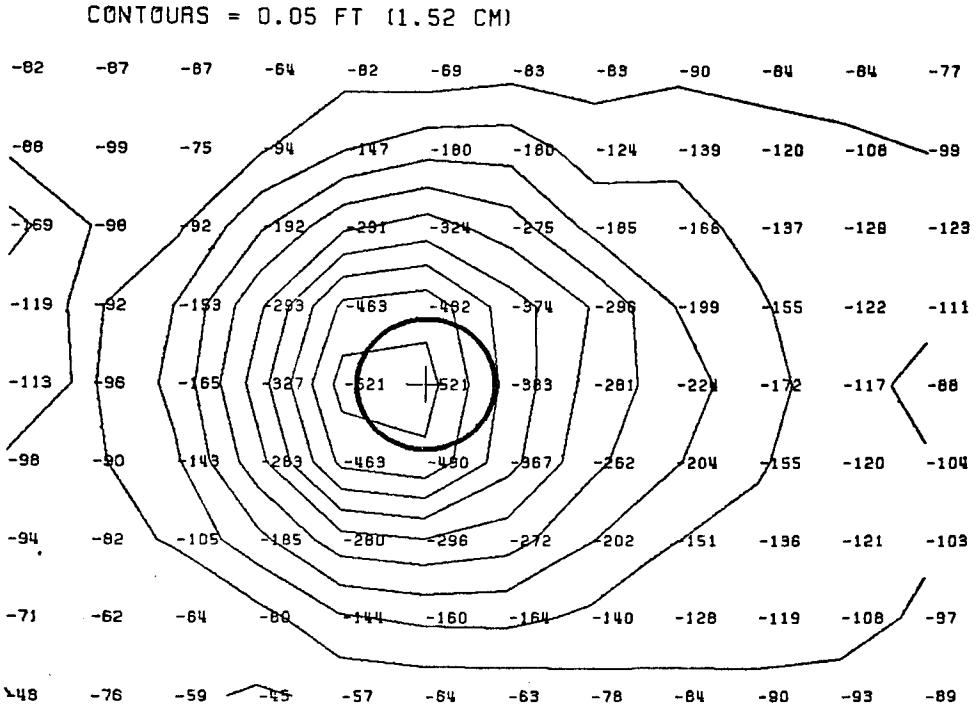

RUN F-3 FR=1.0 Y/B=1 D50=0.25MM 4-INCH PIER

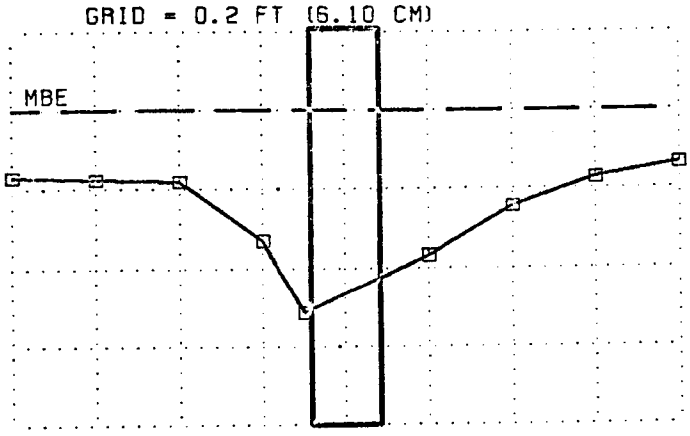

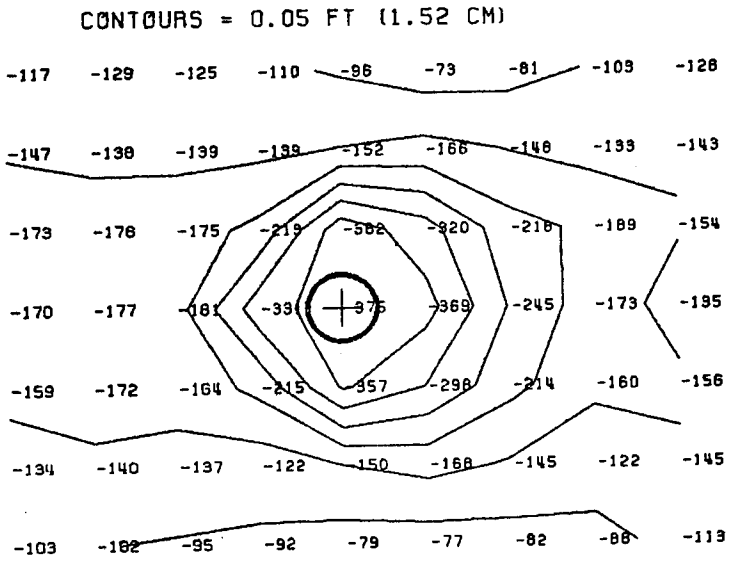

RUN F-4 FR=1.2 Y/B=2 D50=0.25MM 2-INCH PIER

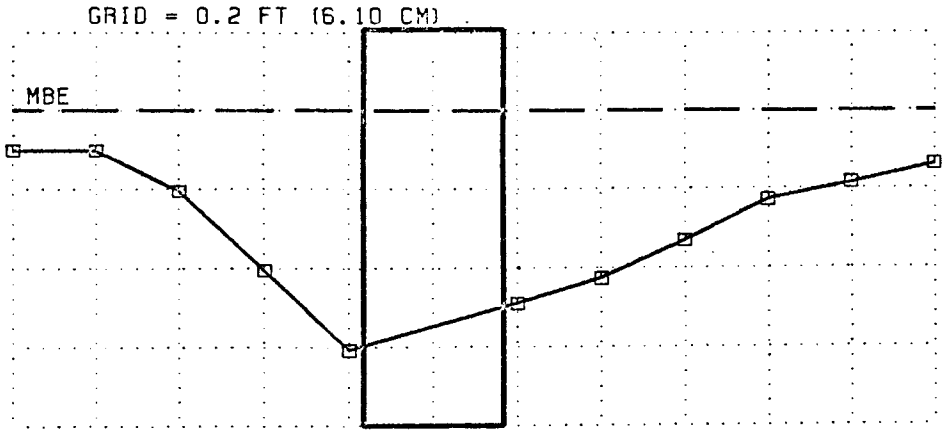

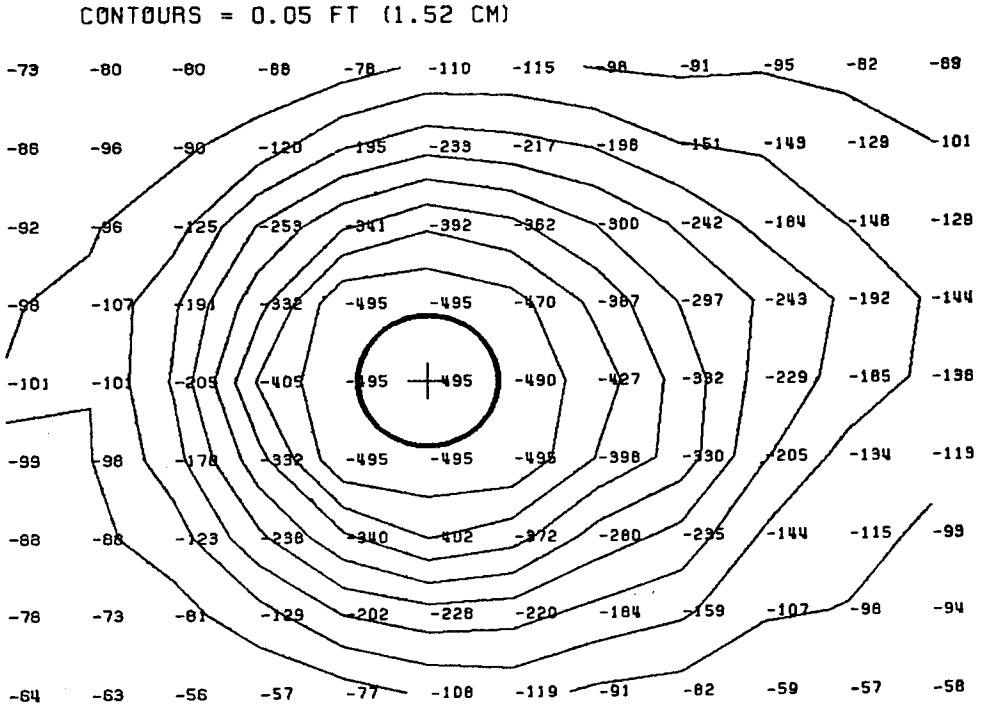

RUN F-4 FR=1.2 Y/B=1 D50=0.25MM 4-INCH PIER

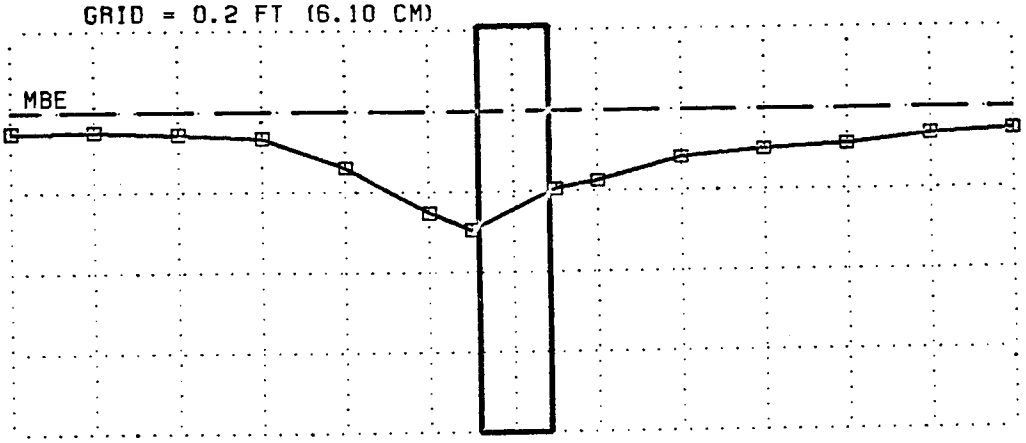

CONTOURS = 0.05 FT (1.52 CM)

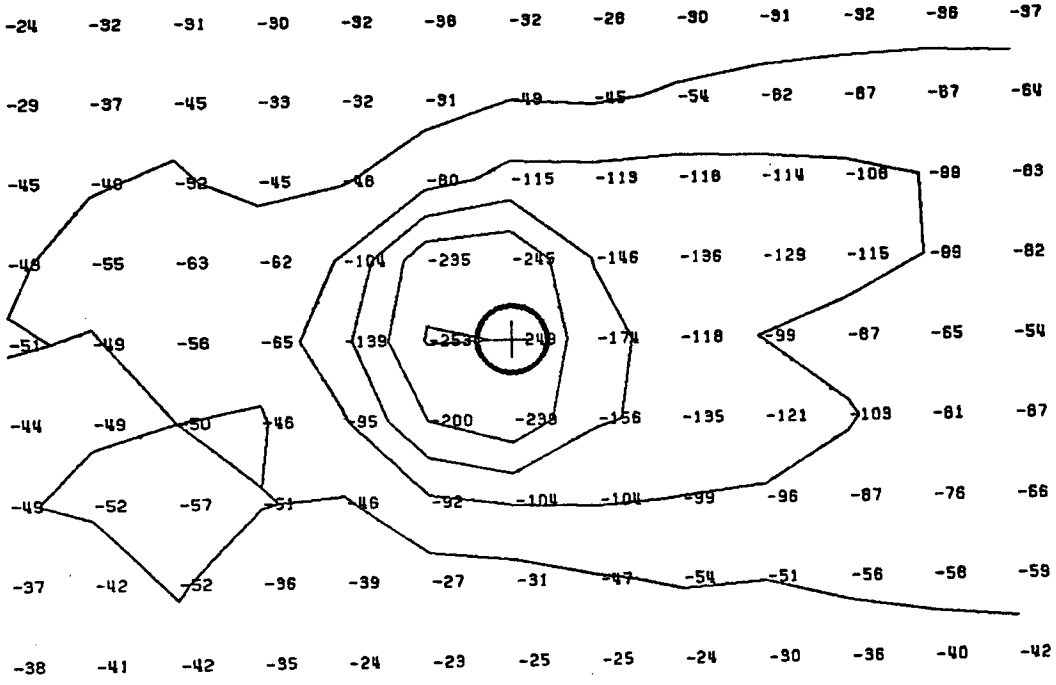

RUN M-1 FR=.5 Y/B=2 D50=1.5MM 2-INCH PIER

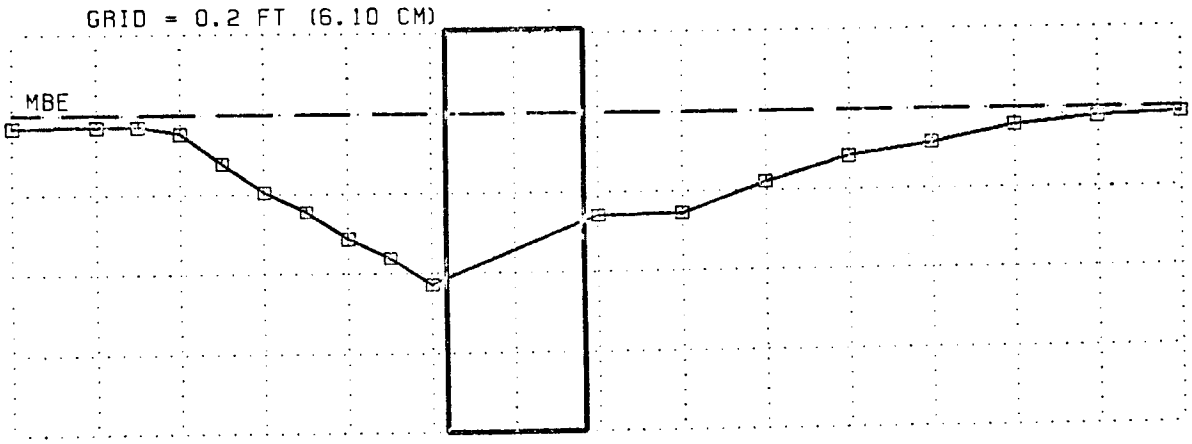

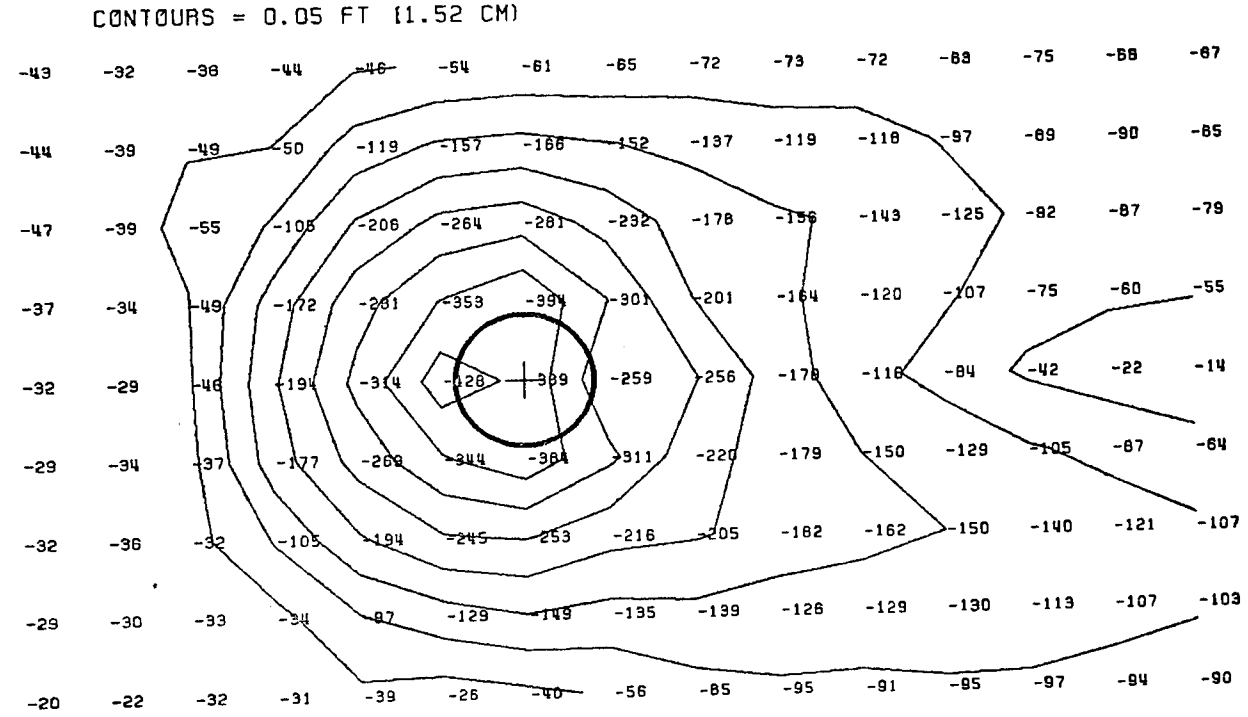

RUN M-1 FR=.5 Y/B=1 D50=1.5MM 4-INCH PIER

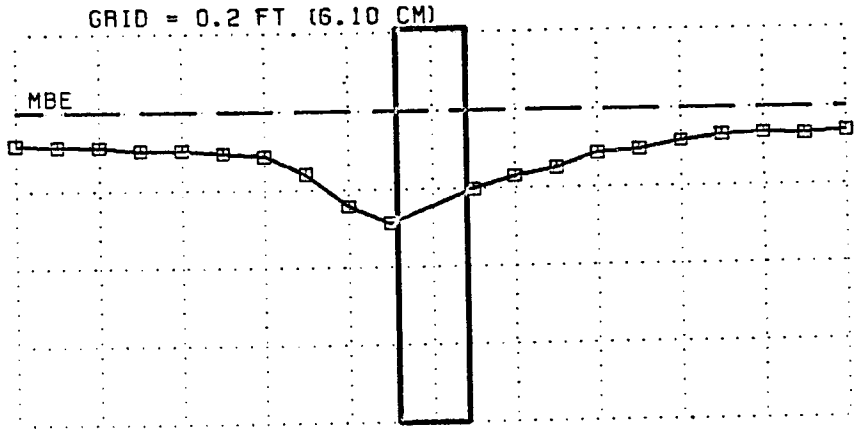

Run M-2 FR=.65 Y/B=2 D50=1.5MM 2-inch pier

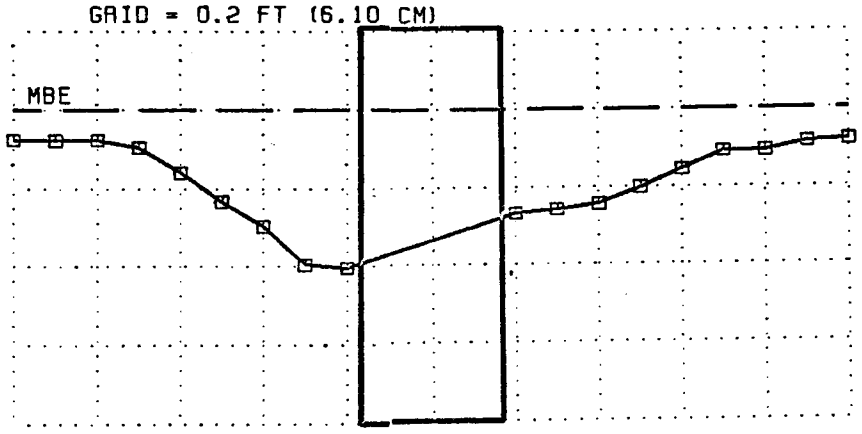

Run M-2 FR=.65 Y/B=1 D50=1.5MM 4-inch pier

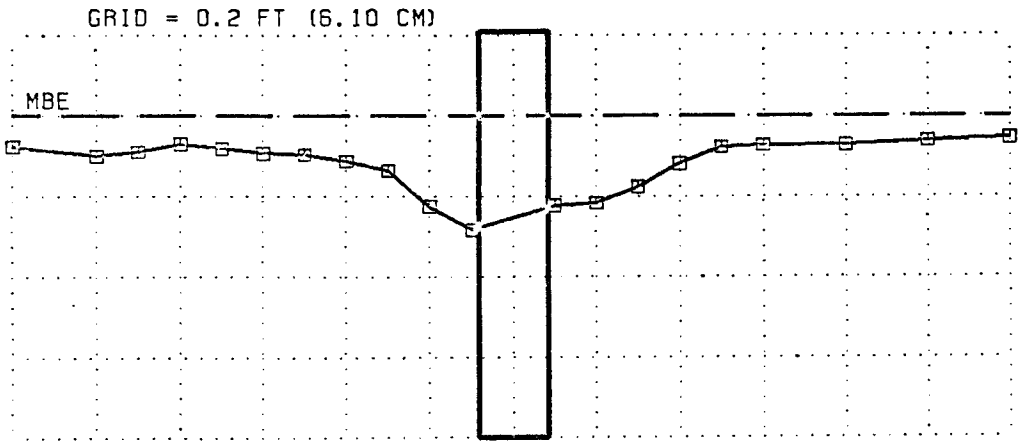

CONTOURS = 0.05 FT (1.52 CM)

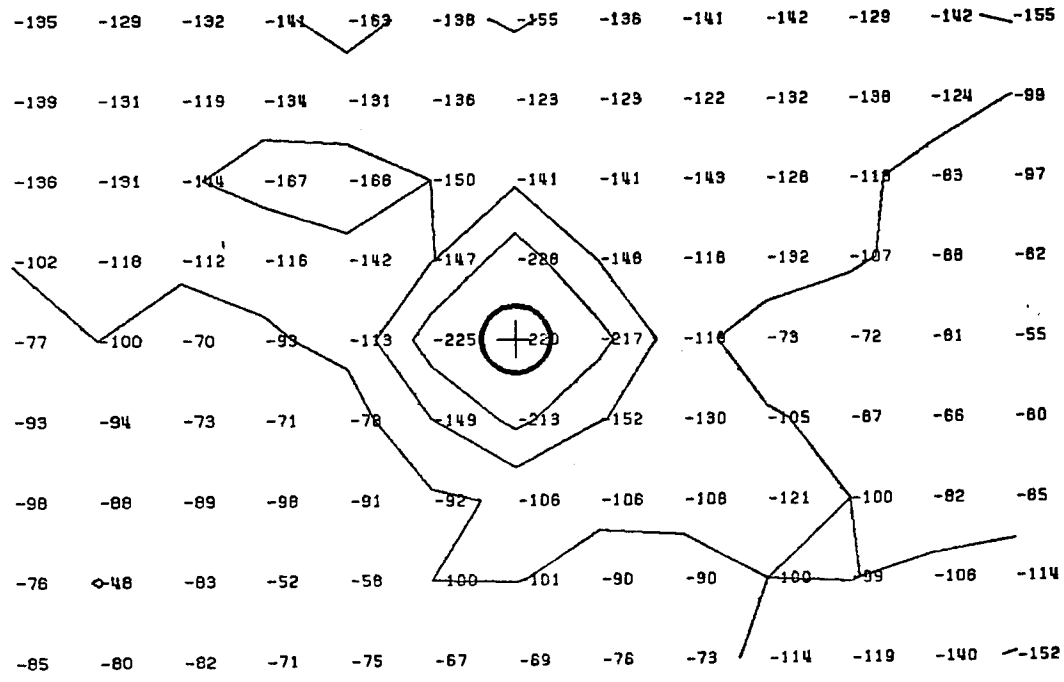

RUN M-3 FR=.75 Y/B=2 D50=1.5MM 2-INCH PIER

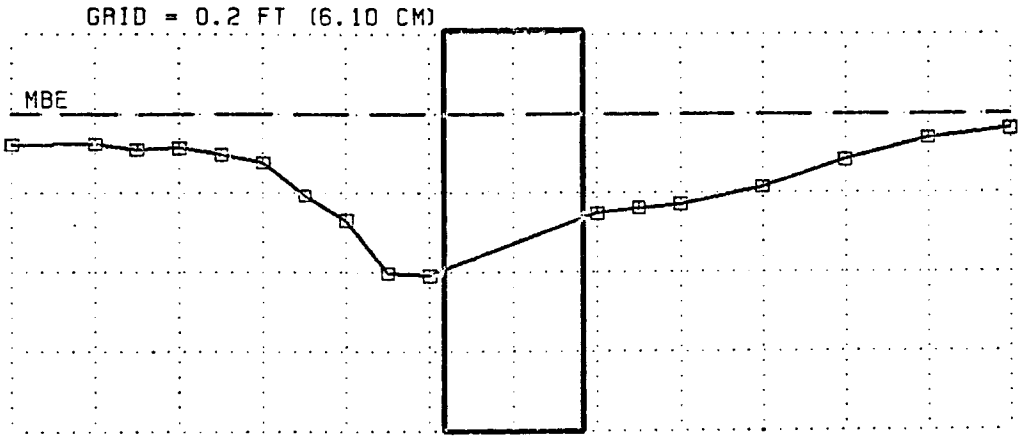

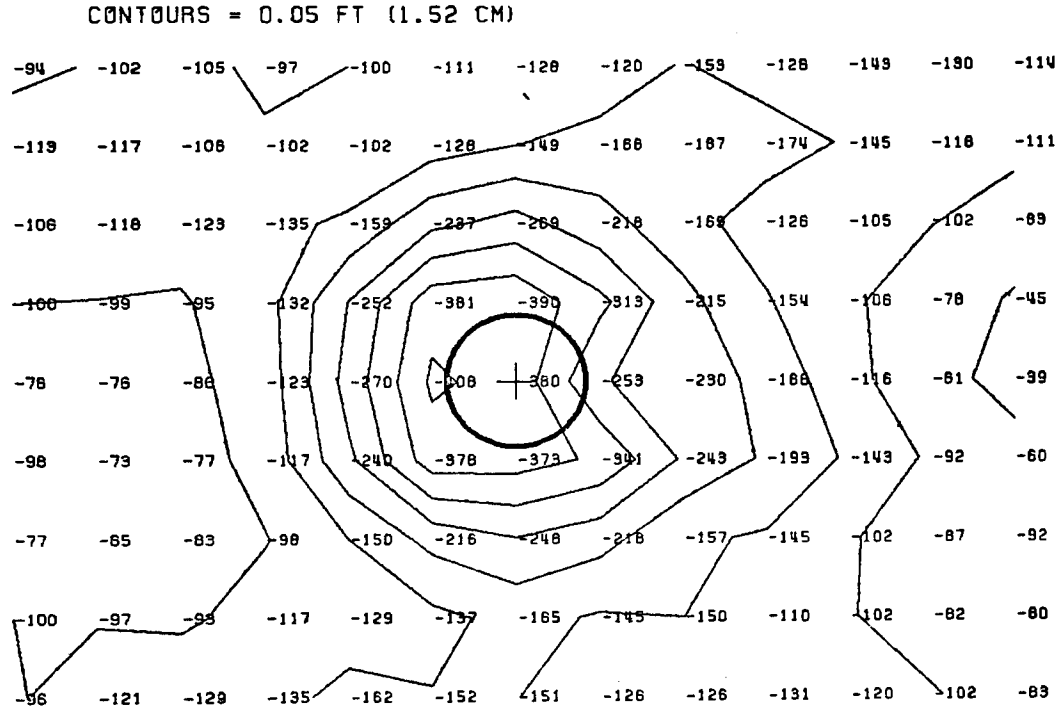

RUN M-3 FR=.75 Y/B=1 D50=1.5MM 4-INCH PIER

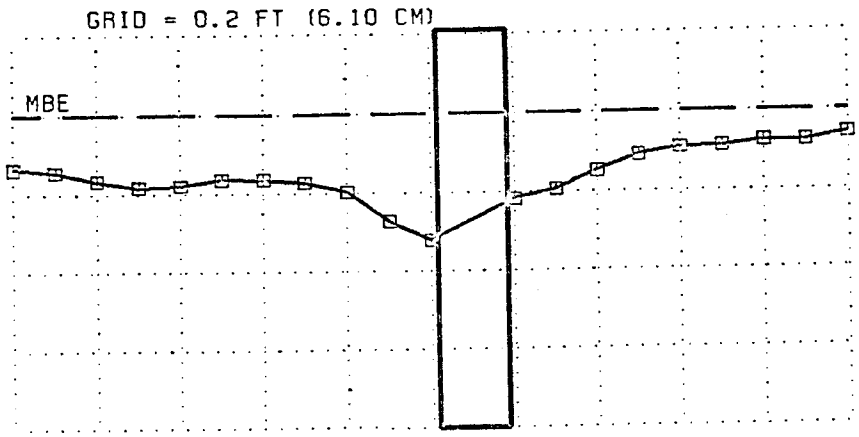

Run M-4 FR=.85 Y/B=2 D50=1.5MM 2-inch pier

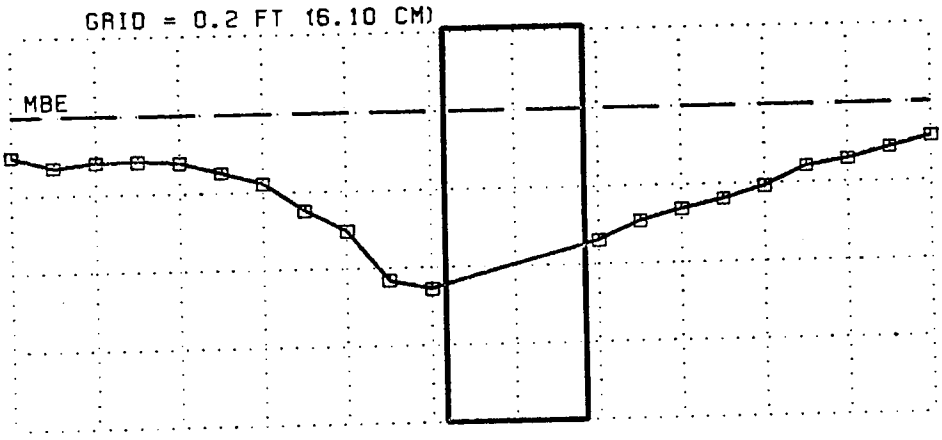

Run M-4 FR=.85 Y/B=1 D50=1.5MM 4-inch pier

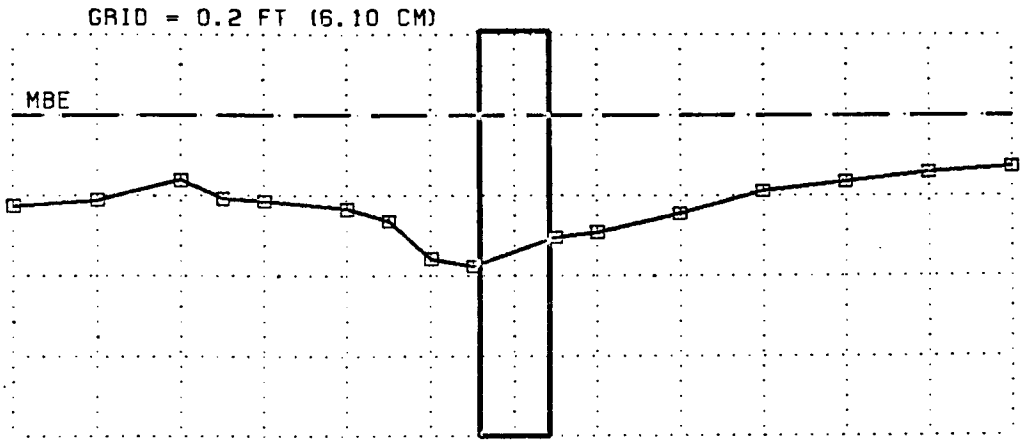

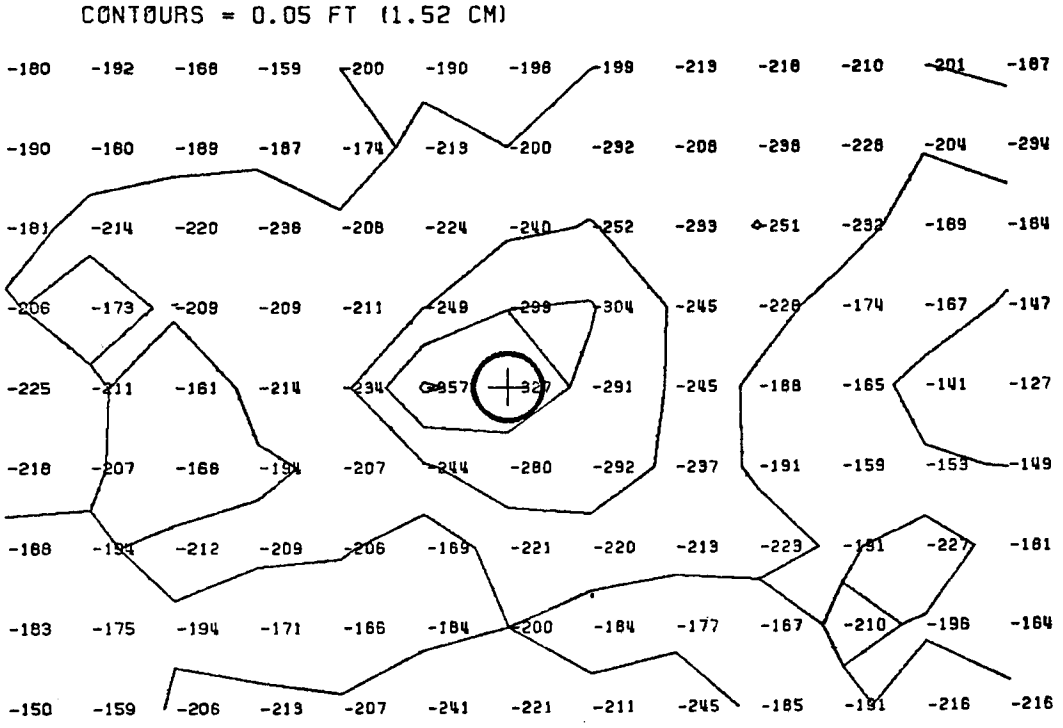

RUN M-5 FR=1.0 Y/B=2 D50=1.5MM 2-INCH PIER

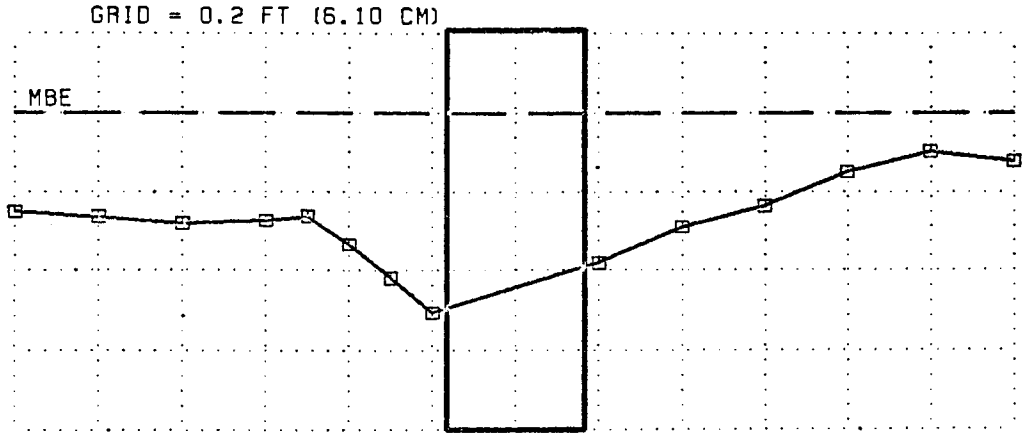

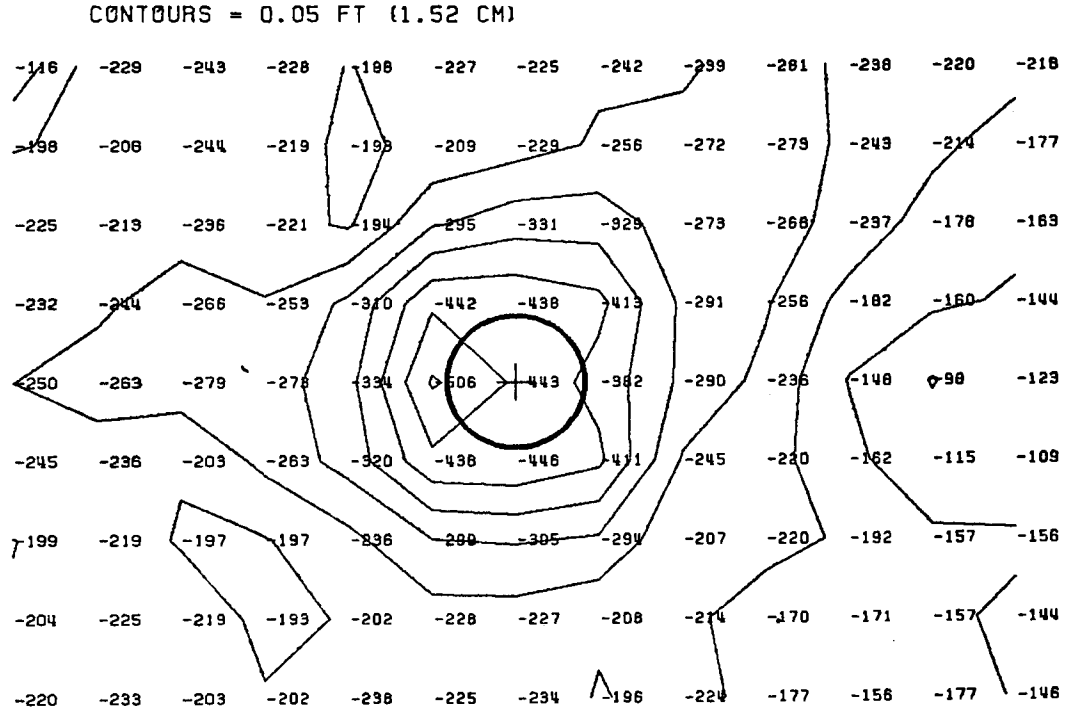

RUN M-5 FR=1.0 Y/B=1 D50=1.5MM 4-INCH PIER

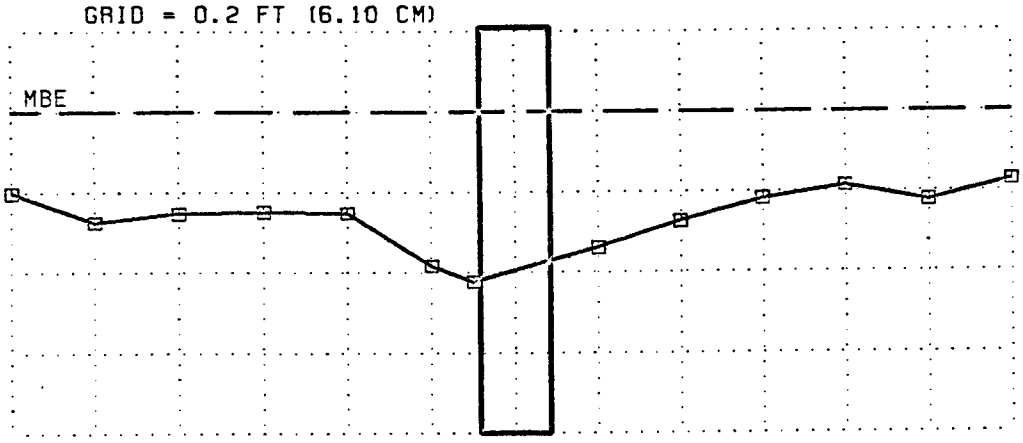

CONTOURS = 0.05 FT (1.52 CM)

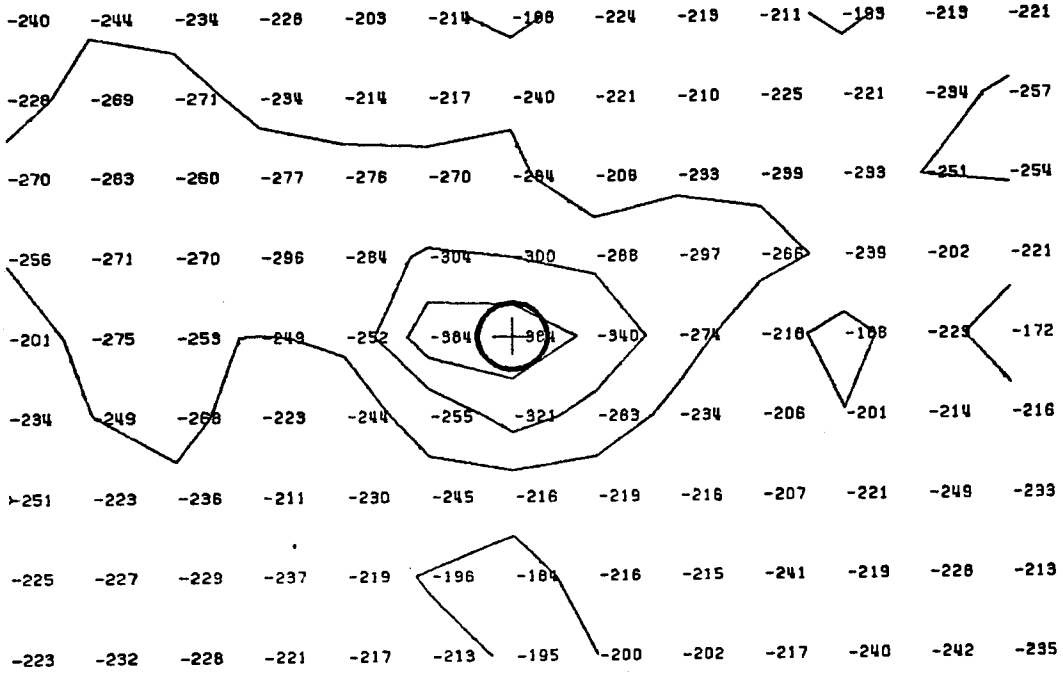

RUN M-6 FR=1.2 Y/B=2 D50=1.5MM 2-INCH PIER

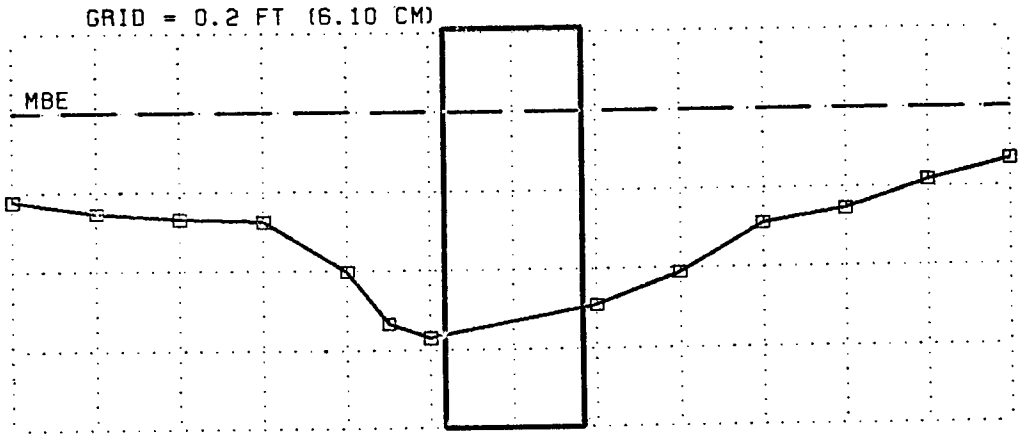

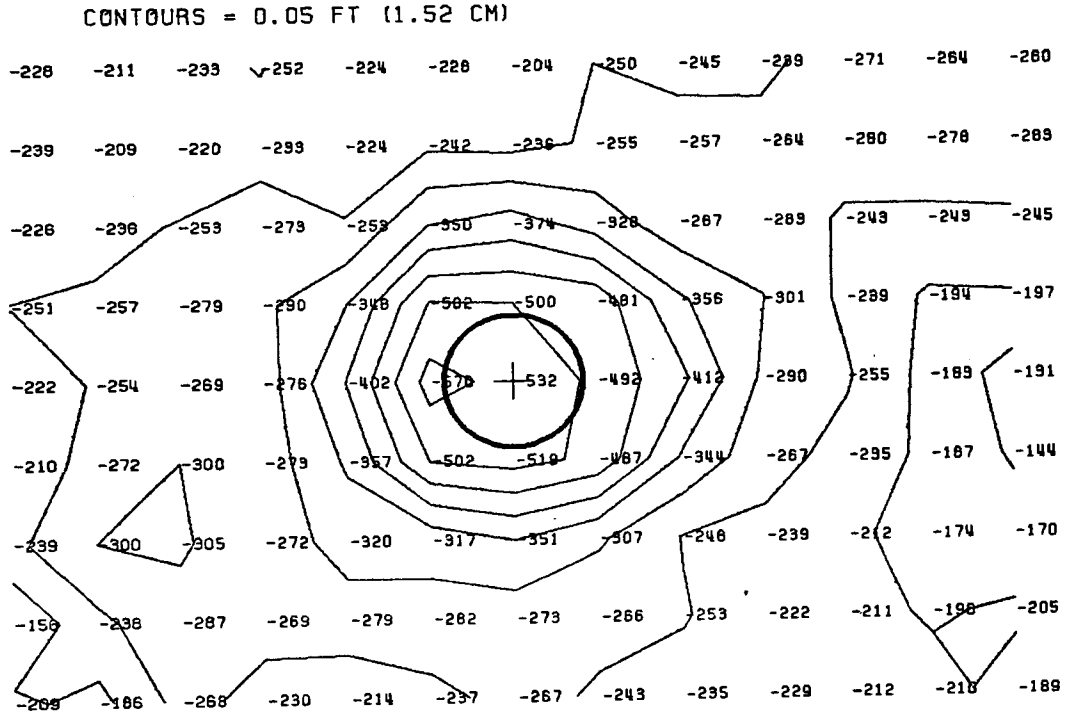

RUN M-6 FR=1.2 Y/B=1 D50=1.5MM 4-INCH PIER

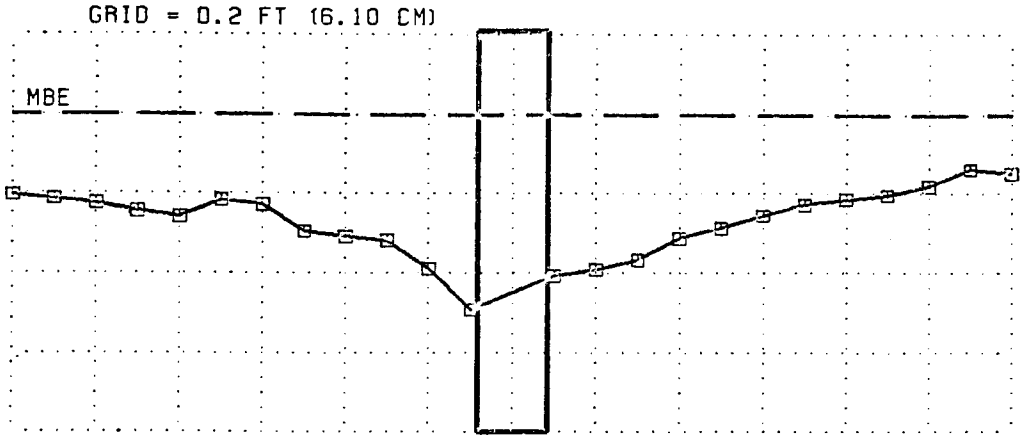

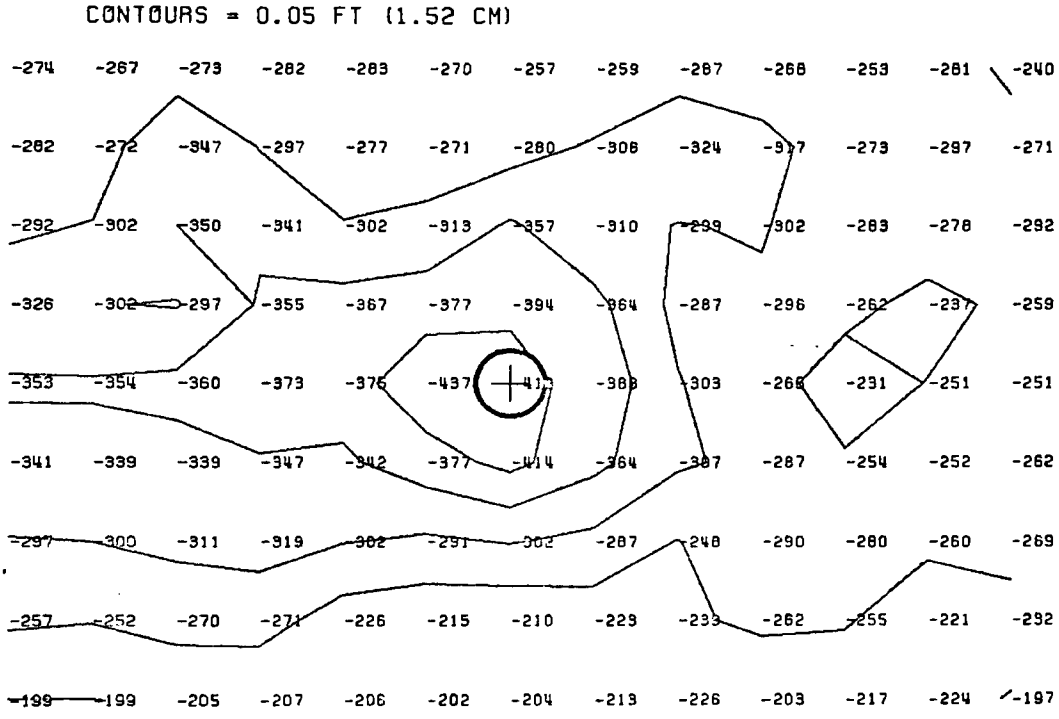

RUN M-7 FR=1.5 Y/B=2 D50=1.5MM 2-INCH PIER

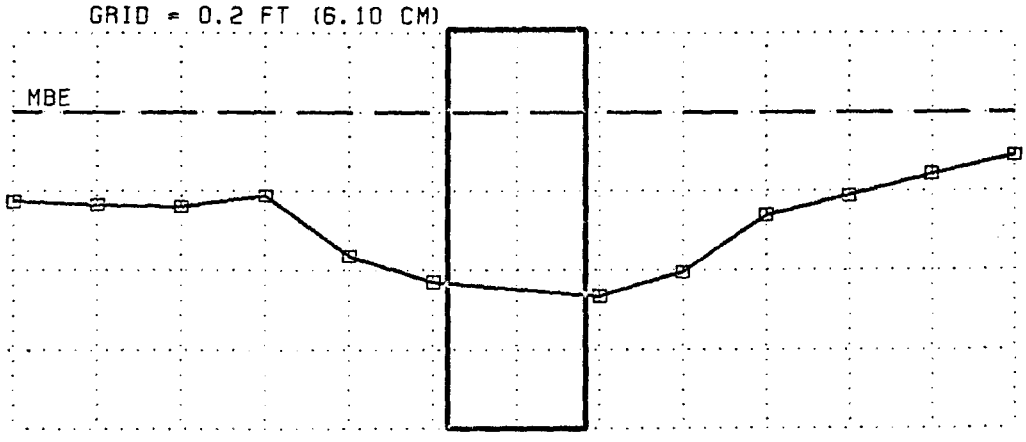

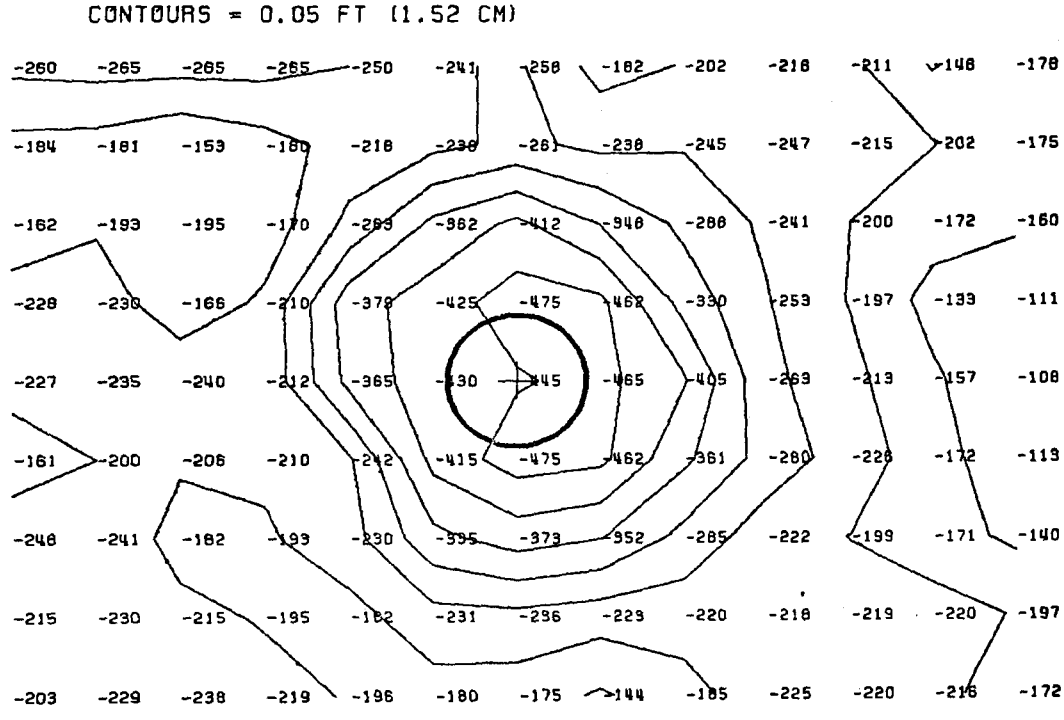

RUN M-7 FR=1.5 Y/B=1 D50=1.5MM 4-INCH PIER

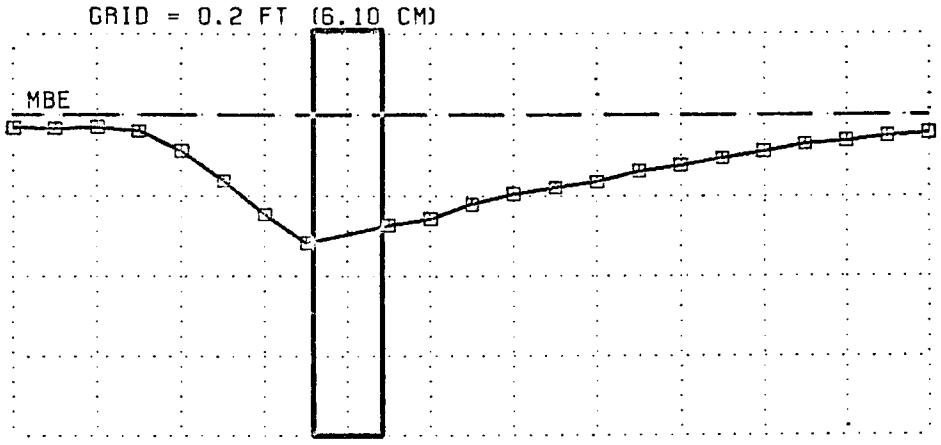

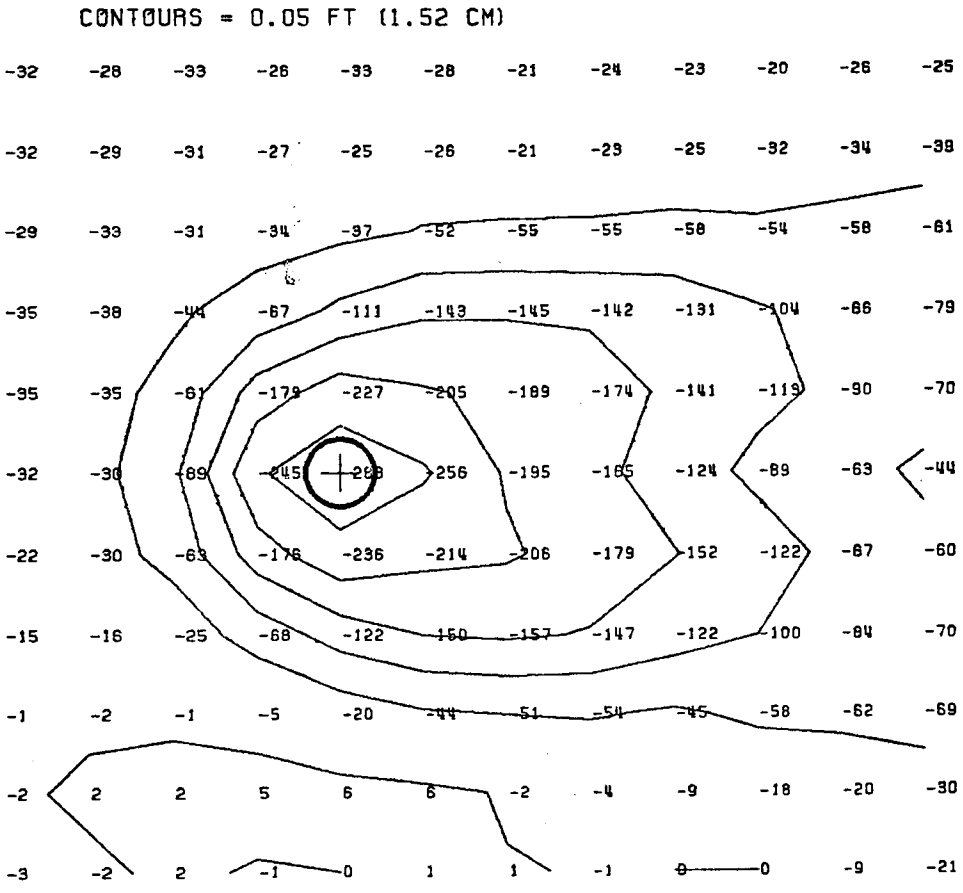

RUN C-1 FR=.5 Y/B=2 D50=2.5MM 2-INCH PIER

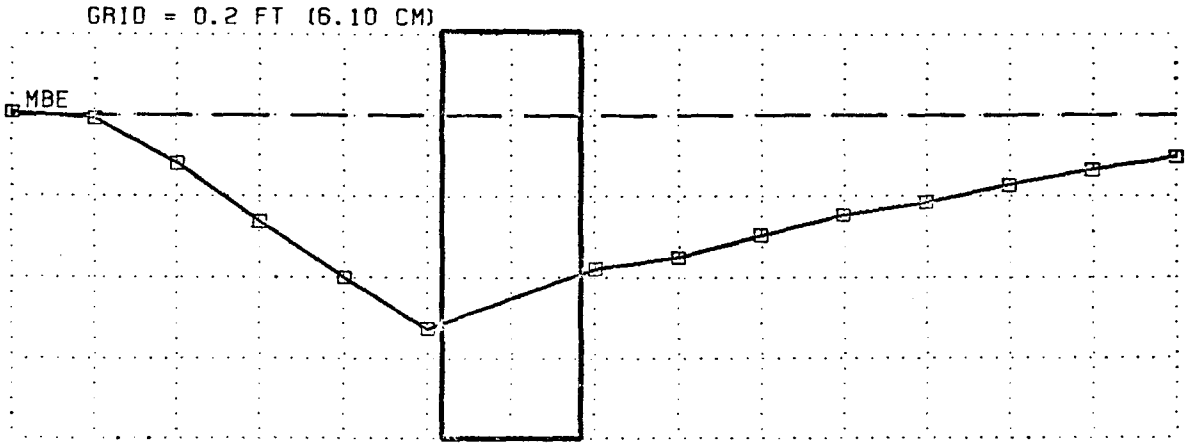

CONTOURS = 0.05 FT (1.52 CM)

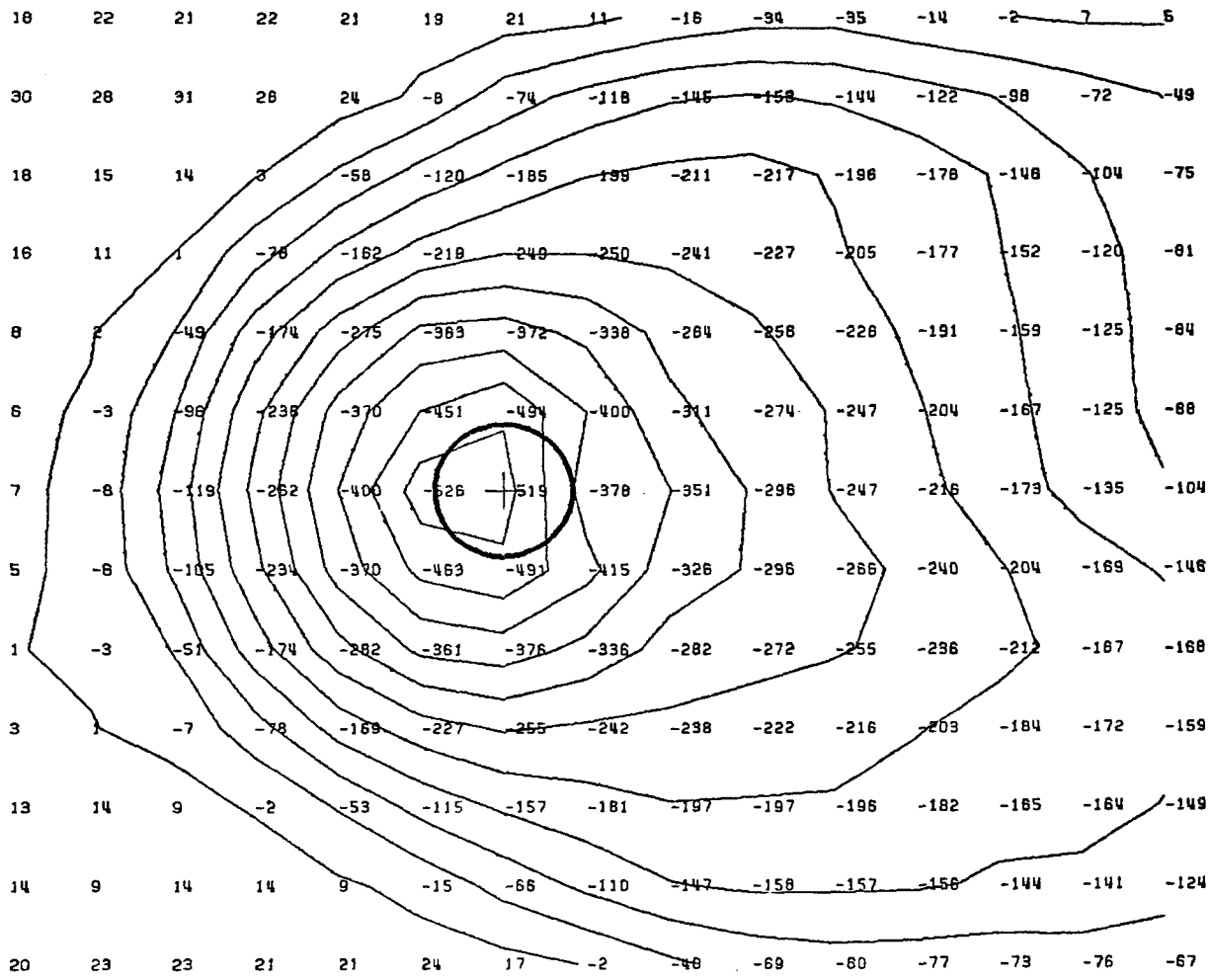

RUN C-1 FR=.5 Y/B=1 D50=2.5MM 4-INCH PIER

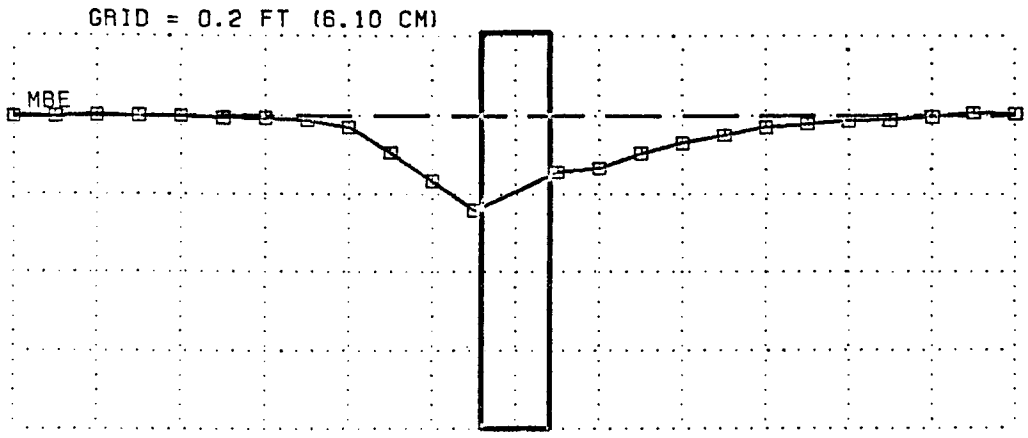

Run C-2 FR=.62 Y/B=2 D50-2.5MM 2-inch pier

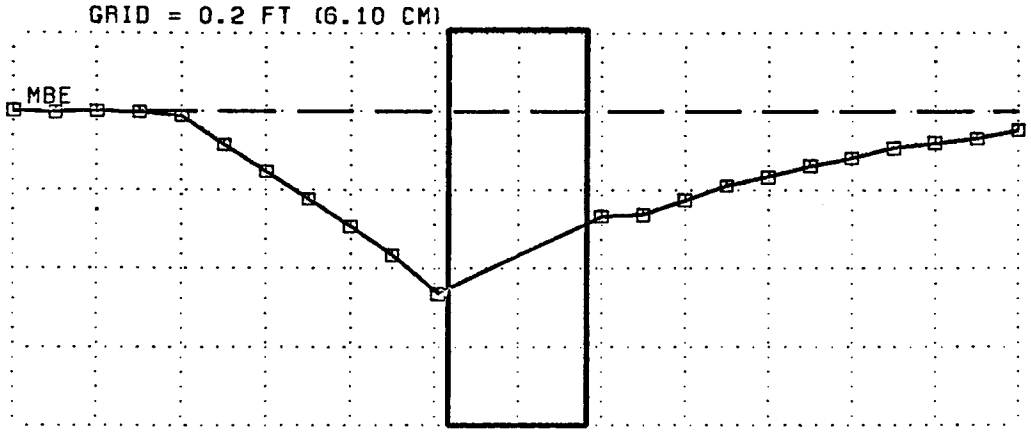

Run C-2 FR=.62 Y/B=1 D50=2.5MM 4-inch pier

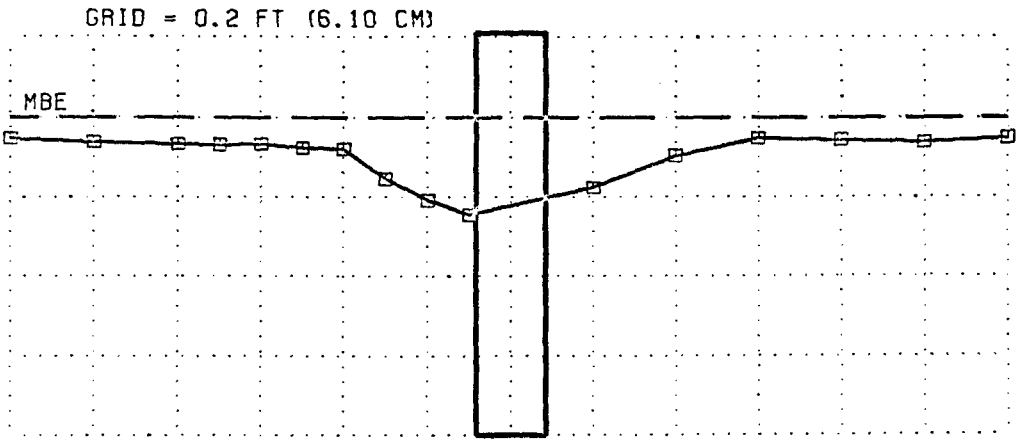

CONTOURS = 0.05 FT (1.52 CM)

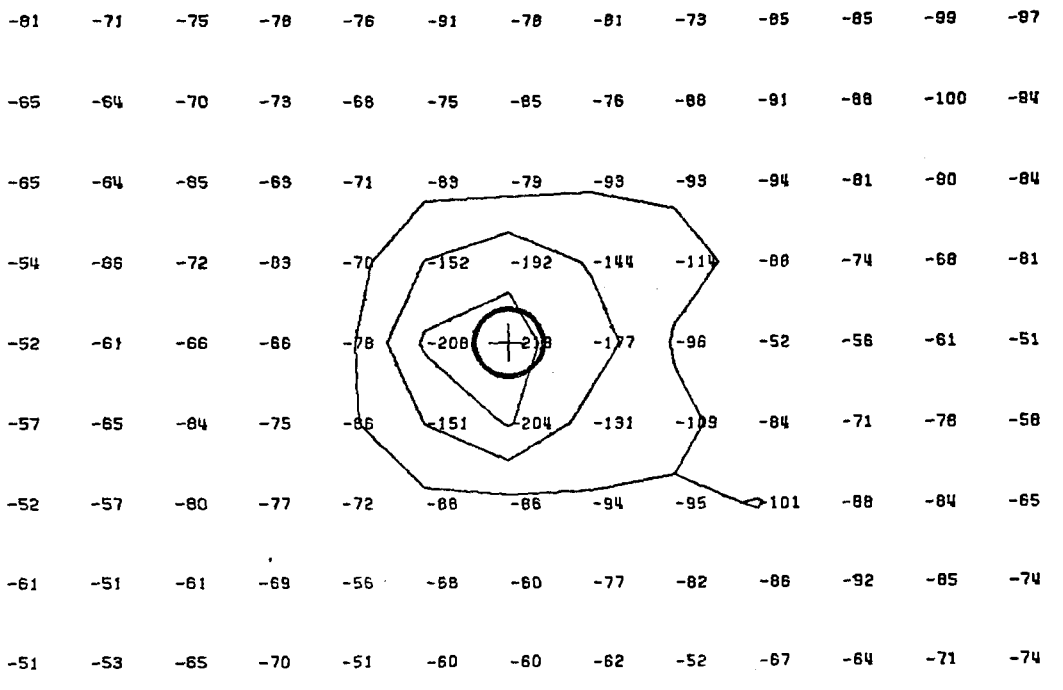

RUN C-3 FR=.75 Y/B=2 D50=2.5MM 2-INCH PIER

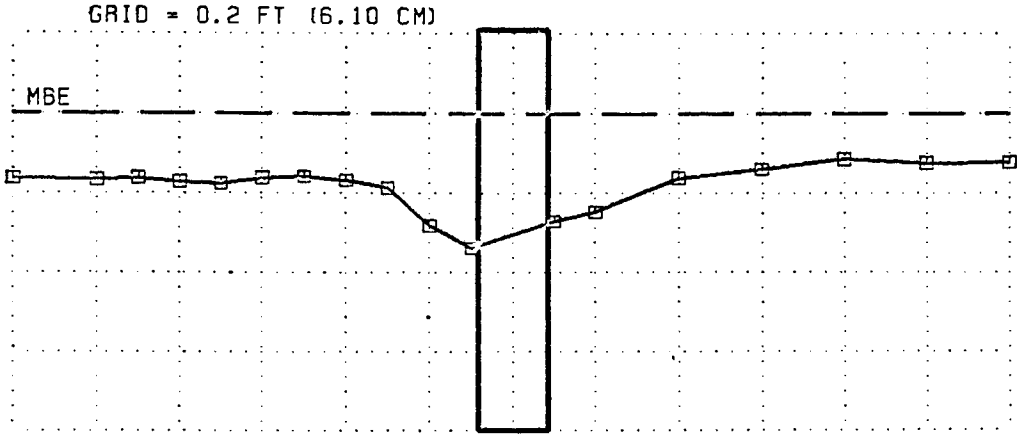

CONTOURS = 0.05 FT (1.52 CM)

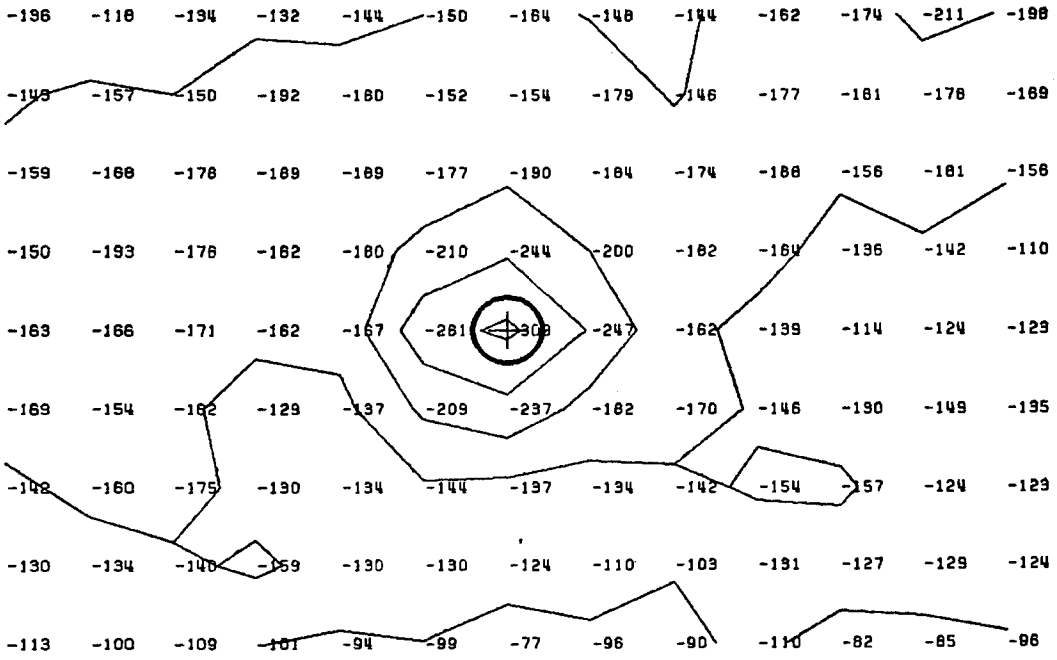

RUN C-4 FR=1.0 Y/B=2 D50=2.5MM 2-INCH PIER

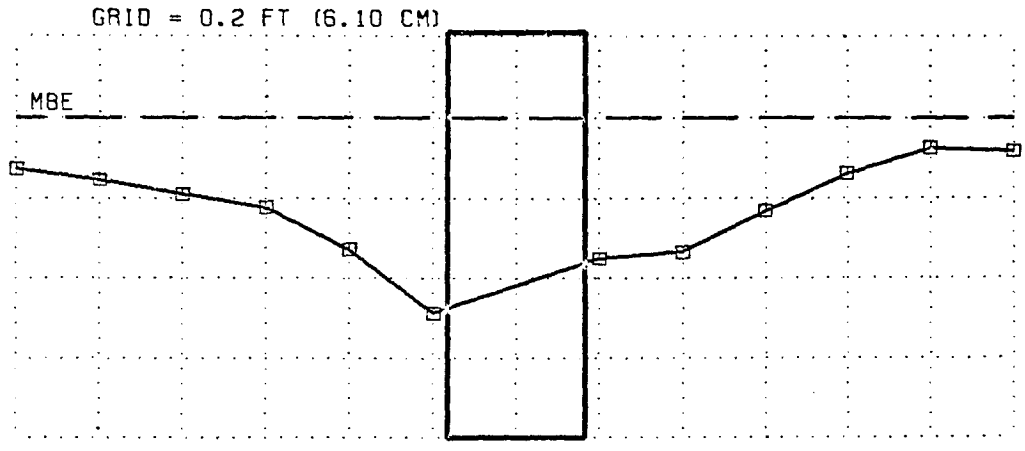

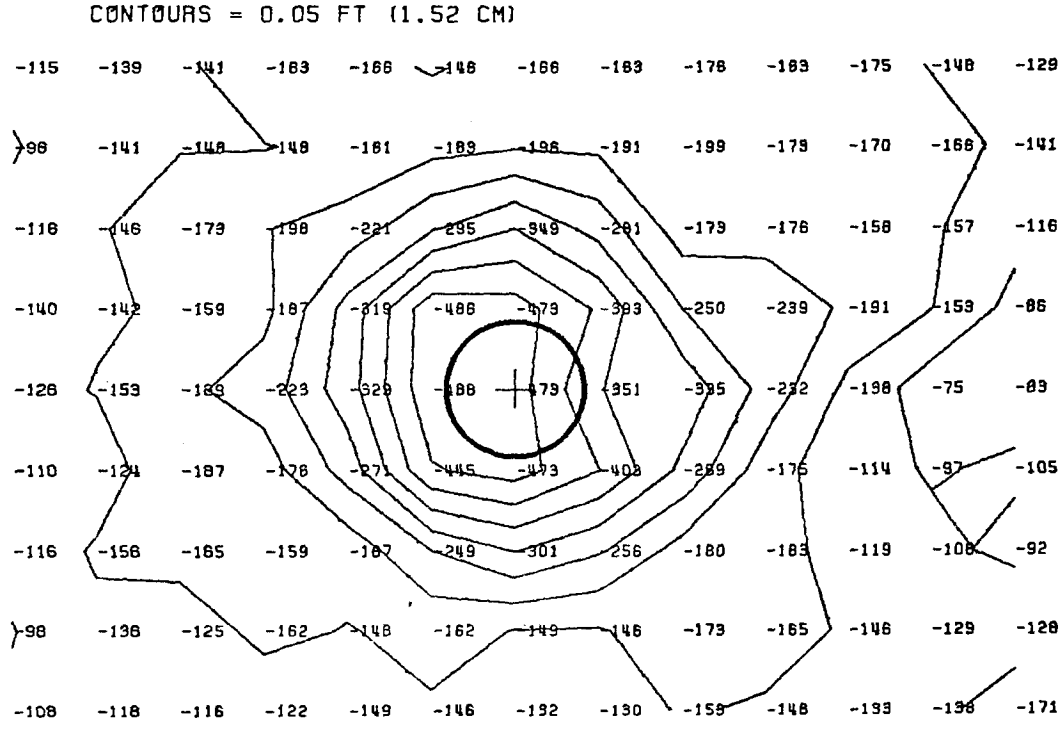

RUN C-4 FR=1.0 Y/B=1 D50=2.5MM 4-INCH PIER

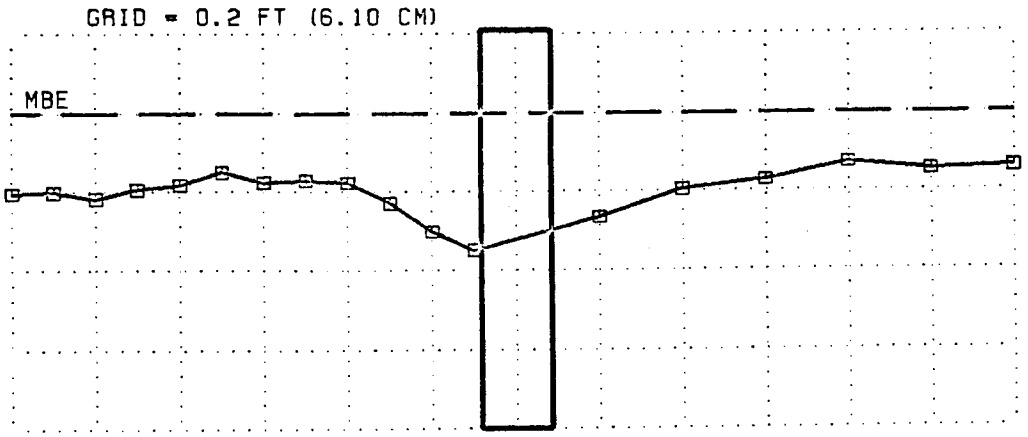

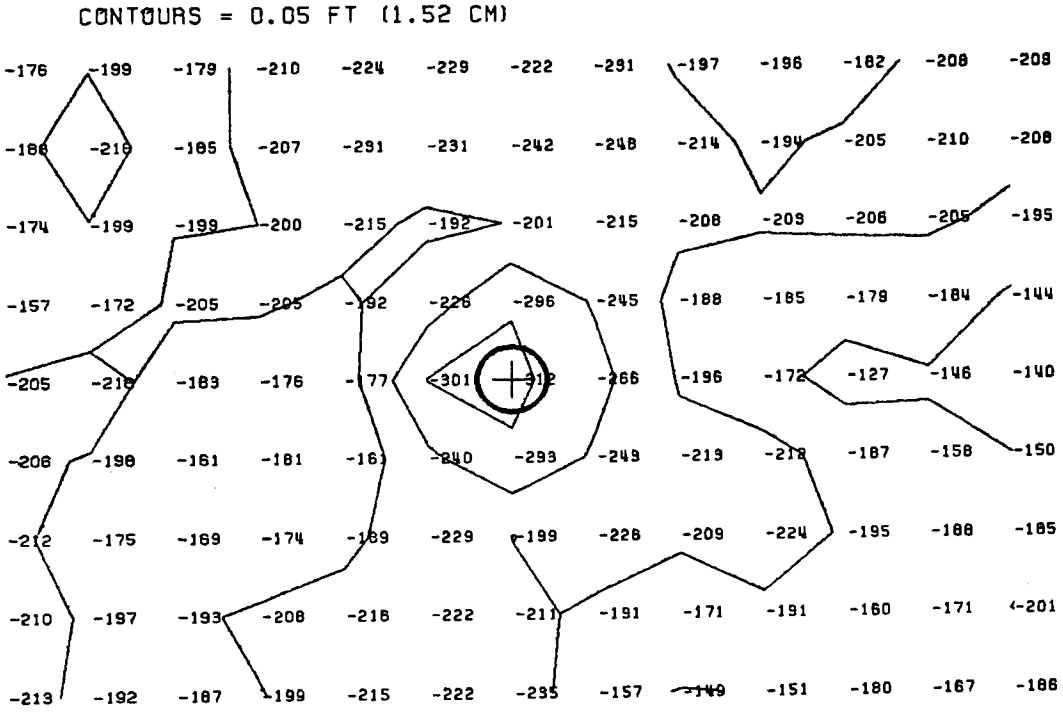

RUN C-5 FR=1.2 Y/B=2 D50=2.5MM 2-INCH PIER

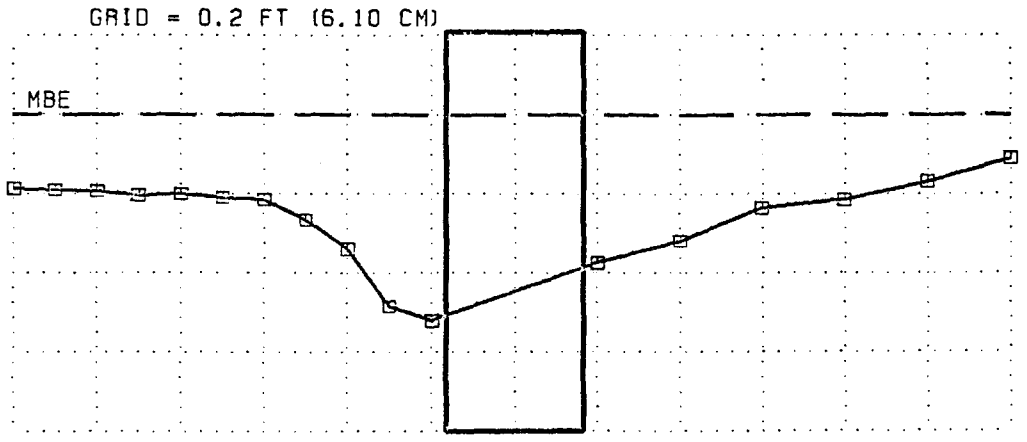

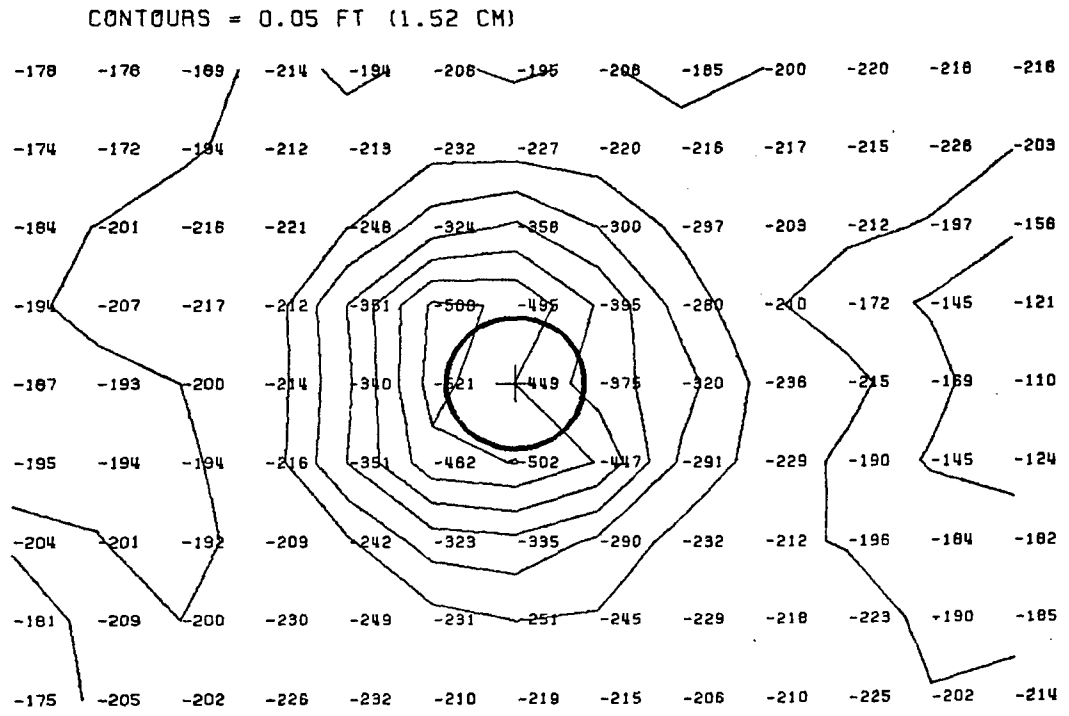

RUN C-5 FR=1.2 Y/B=1 D50=2.5MM 4-INCH PIER